Specific loss of ABCA1 (ATP-Binding Cassette Transporter A1) suppresses TCR (T-Cell Receptor) signaling and provides protection against atherosclerosis

Zhao, Y.; Zhang, L.; Liu, L.; Zhou, X.; Ding, F.; Yang, Y.; ... ; Wang, J.

Arteriosclerosis, Thrombosis, and Vascular Biology

BASIC SCIENCES

Specific Loss of ABCA1 (ATP-Binding Cassette Transporter A1) Suppresses TCR (T-Cell Receptor) Signaling and Provides Protection Against Atherosclerosis

Ying Zhao, Lili Zhang, Limin Liu, Xuan Zhou, Fangfang Ding, Yan Yang, Shiyu Du, Hongmin Wang, Miranda Van Eck, Jun Wang

BACKGROUND: ABCA1 (ATP-binding cassette transporter A1) mediates cholesterol efflux to apo AI to maintain cellular cholesterol homeostasis. The current study aims to investigate whether T-cell–specific deletion of ABCA1 modulates the phenotype/function of T cells and the development of atherosclerosis.

METHODS: Mice with T-cell–specific deletion of ABCA1 on low-density lipoprotein receptor knockout (*Ldlr*$^{-/-}$) background (*Abca1*$^{CD4-/CD4-}$*Ldlr*$^{-/-}$) were generated by multiple steps of (cross)-breedings among *Abca1*$^{flox/flox}$, CD4-*Cre,* and *Ldlr*$^{-/-}$ mice.

RESULTS: Deletions of ABCA1 greatly suppressed cholesterol efflux to apo AI but slightly reduced membrane lipid rafts on T cells probably due to the upregulation of ABCG1. Moreover, ABCA1 deficiency impaired TCR (T-cell receptor) signaling and inhibited the survival and proliferation of T cells as well as the formation of effector memory T cells. Despite the comparable levels of plasma total cholesterol after Western-type diet feeding, *Abca1*$^{CD4-/CD4-}$*Ldlr*$^{-/-}$ mice showed significantly attenuated arterial accumulations of T cells and smaller atherosclerotic lesions than *Abca1*$^{+/+}$*Ldlr*$^{-/-}$controls, which were associated with reduced surface CCR5 (CC motif chemokine receptor 5) and CXCR3 (CXC motif chemokine receptor 3), decreased antiapoptotic Bcl-2 (B-cell lymphoma 2) and Bcl-xL (B-cell lymphoma extra-large), and hampered abilities to produce IL (interleukin)-2 and IFN (interferon)-γ by ABCA1-deficient T cells.

CONCLUSIONS: ABCA1 is essential for T-cell cholesterol homeostasis. Deletion of ABCA1 in T cells impairs TCR signaling, suppresses the survival, proliferation, differentiation, and function of T cells, thereby providing atheroprotection in vivo.

GRAPHIC ABSTRACT: A graphic abstract is available for this article.

Key Words: apoptosis ■ atherosclerosis ■ cell movement ■ cholesterol ■ interferon-gamma ■ memory T cells

ABCA1 (ATP-binding cassette transporter A1) is a plasma membrane protein and functions as a major regulator of cellular cholesterol homeostasis by promoting the efflux of cholesterol to lipid-free/poor apo AI.[1] Loss-of-function mutations of ABCA1 cause Tangier's disease characterized by low plasma HDL (high-density lipoprotein), increased cholesterol ester accumulation and deposition in macrophages, and premature atherosclerosis.[2] Likewise, total-body deletion of ABCA1 in mice leads to the virtual absence of HDL and enhanced macrophage foam cell formation.[3] As such, targeted depletions of ABCA1 in specific cells/organs of mice have been instrumental in deciphering its biological functions in a cell/organ-specific manner. Selective deletion of ABCA1 in liver, intestine, or adipose tissue revealed that ABCA1-dependent cholesterol efflux from the liver is a major determinant of HDL biogenesis, whereas intestinal and adipocyte ABCA1 also contributes significantly

Correspondence to: Ying Zhao, PhD, Department of Pathophysiology, School of Biology & Basic Medical Sciences, Soochow Medical College of Soochow University, Suzhou, 215123 China, Email yzhao@suda.edu.cn; or Jun Wang, PhD, Institutes of Biology & Medical Sciences, Soochow Medical College of Soochow University, Suzhou, 215123 China, Email jwang79@suda.edu.cn

Supplemental Material is available at https://www.ahajournals.org/doi/suppl/10.1161/ATVBAHA.122.318226.
For Sources of Funding and Disclosures, see page e325.

Arterioscler Thromb Vasc Biol is available at www.ahajournals.org/journal/atvb

Nonstandard Abbreviations and Acronyms

ABCA1	ATP-binding cassette transporter A1
ABCG1	ATP-binding cassette transporter G1
EM	effector memory
HDL	high-density lipoprotein
LDLr	low-density lipoprotein receptor
LXR	liver X receptor
MFI	mean fluorescence intensity
NLD	normal laboratory diet
TCR	T-cell receptor
Treg	regulatory T cells
WTD	western-type diet

to the circulating HDL pool.[4–6] Moreover, studies in which ABCA1-deficient bone marrow was transplanted into atherosclerosis-susceptible low-density lipoprotein receptor knockout (*Ldlr*$^{-/-}$) mice showed that ABCA1 in bone marrow–derived cells prevents macrophage foam cell formation and reduces atherosclerosis susceptibility without affecting plasma levels of HDL-C (HDL cholesterol).[3,7,8] Similarly, hematopoietic overexpression of human ABCA1 attenuates the development of atherosclerosis.[9] As bone marrow–derived monocytes/macrophages are the major precursors for foam cells in atherosclerotic lesions, macrophage ABCA1 was supposed to be atheroprotective. However, a minimal contribution of macrophage ABCA1 to atherogenesis has been noted in studies using myeloid-specific lysozyme M promotor-driven deletion of ABCA1 in *Ldlr*$^{-/-}$ mice.[10,11] These findings suggest that the atheroprotective effects of hematopoietic ABCA1 are largely mediated via other bone marrow–derived cells than mature macrophages or neutrophils.

Given the increased amounts of peripheral lymphocytes in animals transplanted with *Abca1*$^{-/-}$ bone marrow,[7,8] Brunham et al hypothesized that the enhanced lymphocytosis might contribute to the increased lesion formation upon deletion of ABCA1 in the hematopoietic system.[10] The development of atherosclerotic lesions under hyperlipidemia is regulated by the balance of effector and regulatory T cells (Treg).[12] Notably, the fitness of both effector and Treg cells strictly relies on cholesterol homeostasis, as cholesterol and its metabolites not only mediate the formation of lipid rafts that facilitate the clustering of signaling molecules (ie, TCR [T-cell receptor])[13,14] but also modulate the activities of many transcription factors (ie, SREBP [sterol regulatory element-binding proteins] and LXR [liver X receptor]).[15,16] Accordingly, ABCG1, an active cholesterol transporter, has been implicated in regulating the cholesterol homeostasis and function of T cells. ABCG1 mediates cholesterol efflux to mature HDL, and its induction by LXR activation suppresses the proliferation of T cells.[15] Moreover, deletion of ABCG1 in T cells has been shown to enhance the formation of lipid rafts, potentiate TCR signaling in CD4$^+$ T cells, and ameliorate atherosclerosis in *Ldlr*$^{-/-}$ mice by promoting the generation of Treg cells.[17,18] By contrast, the roles of ABCA1 in T-cell cholesterol homeostasis and function as well as in atherosclerotic lesion development remain largely unknown.

Highlights

- T cells depend on ABCA1 (ATP-binding cassette transporter A1) for cholesterol efflux to apo AI and small dense HDL (high-density lipoprotein).
- T-cell–specific deletion of ABCA1 impairs their TCR (T-cell receptor) signaling, survival and proliferation and reduces the formation and functions of effector memory T cells in hypercholesterolemic *Ldlr*$^{-/-}$ mice.
- Specific deletion of ABCA1 in T cells provides protection against atherosclerosis.

In the present study, we generated mice specifically lacking ABCA1 in T cells and showed that ABCA1 is crucial for cholesterol homeostasis and modulates TCR signaling in both CD4$^+$ and CD8$^+$ T cells. Strikingly, targeted deletion of ABCA1 in T cells reduces the membrane content of lipid rafts, impairs the TCR signaling, suppresses the formation and function of effector memory (EM) T cells, and mitigates the accumulation of T cells in atherosclerotic lesions, thereby providing atheroprotection in vivo.

MATERIALS AND METHODS

Data Availability

The majority of data supporting the findings of this study are presented within the article and its Supplemental Material. Data that are not directly included are available from the corresponding author upon reasonable request.

Mice and Diet

Abca1$^{fl/fl}$*Abcg1*$^{fl/fl}$ (The Jackson Laboratory, catalog 021067) and *CD4-Cre* (kindly provided by Professor Zichun Hua, Nanjing University) mice were first crossed with *Ldlr*$^{-/-}$ mice (T001464; Nanjing Biomedical Research Institute of Nanjing University) to generate *Abca1*$^{fl/fl}$*Ldlr*$^{-/-}$ and *CD4-Cre*$^+$*Ldlr*$^{-/-}$mice, respectively. *Abca1*$^{fl/fl}$*Ldlr*$^{-/-}$ mice were subsequently crossed with *CD4-Cre*$^+$*Ldlr*$^{-/-}$ to obtain *CD4-Cre*$^+$*Abca1*$^{fl/fl}$*Ldlr*$^{-/-}$ (*Abca1*$^{CD4-/CD4-}$*Ldlr*$^{-/-}$) and the control *CD4-Cre*$^-$*Abca1*$^{fl/fl}$*Ldlr*$^{-/-}$ (*Abca1*$^{+/+}$*Ldlr*$^{-/-}$) mice for in vivo atherosclerosis studies. OT-II TCR transgenic mice (kindly provided by Prof. Haopeng Wang, ShanghaiTech University) were used to generate *CD4-Cre*$^+$*Abca1*$^{fl/fl}$OT-II and control *CD4-Cre*$^-$*Abca1*$^{fl/fl}$OT-II mice. CD45.1 congenic mice were obtained from Professor Jingping Zhang (Soochow University). All mice were on a C57BL/6J background and maintained on sterilized normal laboratory diet (NLD, MD17121; Medicience) containing 4.3% (w/w) fat with no added cholesterol under specific-pathogen-free conditions. At the age of 10 to 12 weeks, male or female *Abca1*$^{CD4-/CD4-}$*Ldlr*$^{-/-}$ mice and

the corresponding *Abca1*$^{+/+}$*Ldlr*$^{-/-}$control littermates received a Western-type diet (WTD) containing 21% (w/w) total fat and 0.15% cholesterol (D12079B, Research Diet) for 9 weeks to induce the formation of atherosclerotic lesions. The sample size calculation for atherosclerotic lesion experiments (n=≈14/group) was based on our pilot data (effect size 65, variability 50, significant level 0.05, power 0.9, and 2-sided test) using the online software (experimental design assistant; https://eda.nc3rs.org.uk/eda/login/auth). *Abca1*$^{CD4-/CD4-}$*Ldlr*$^{-/-}$ and control littermates were co-housed at the ratio of ≈1:1 and were free to get access to food and water in the cage. No exclusion and randomization were performed during the experiment. Animal experiments were conducted in accordance with the protocols approved by the Soochow University Institutional Animal Care and Use Committee.

Plasma Lipid Analyses

After an overnight fasting period, 100 µL of blood was drawn from the mice by tail bleeding. The concentrations of cholesterol in sera were determined by incubation with 0.025 U/mL cholesterol oxidase (228250; Calbiochem), 0.065 U/mL peroxidase (P2088; Sigma), and 15 µg/mL cholesteryl esterase (228180; Calbiochem) in reaction buffer (1.0 KPi buffer, pH=7.7 containing 0.01 M phenol, 1 mM 4-amino-antipyrine, 1% polyoxyethylene-9-laurylether and 7.5% methanol). Absorbance was read at 490 nm.

Histological Analysis of Atherosclerosis

On euthanization, the arterial tree was perfused in situ with PBS and the heart was excised and immediately stored in 3.7% neutral-buffered formalin until use. The hearts were bisected just below the atria and transferred into a renumbered tube by one investigator, and the base of the hearts plus aortic roots were embedded in optical coherence tomography for analysis by another investigator with no information on the genotypes. The hearts were then cryosectioned perpendicular to the axis of the aorta, starting within the heart and working in the direction of the aortic arch as described before.[17,18] Once the first 2 aortic valves appeared, serial 10-µm sections were taken alternately on three slides (5 sections/slide) per group for total of 4 to 5 groups until the disappearance of the 3 aortic valve leaflets. Three slides/aortic roots from 3 continuous groups that contained 15 cross-sections were stained with oil-red-O to visualize lesions. To keep consistency for lesion quantification in the same location for each aortic root, we used the appearance of the 3 aortic valve leaflets as the start point and consecutive 10 sections right after that were measured. The atherosclerotic lesion area in sections was quantified using the Nikon image analysis system, consisting of a Nikon CiS microscope coupled to a video camera DS-Fi1 and NIS Elements Imaging software (Nikon Ltd). One slide/aortic root from the same location was immunostained with the α-MOMA-2 (MCA519; AbD Serotec) and α-CD3 (ab16669; Abcam) antibody, respectively, with the inclusion of rat or rabbit IgG as corresponding isotype controls. The MOMA-2–positive lesion areas were subsequently quantified as percent of total lesions in 5 consecutive sections by computer-aided morphometric analysis using NIS Elements Imaging analysis system. All analyses were performed blinded.

Isolation of Cells

At euthanization, white blood cells in peripheral blood were obtained by removing red blood cells with RBC Lysis buffer (64010-00-100, Biogems). Spleens, thymuses, and aorta-draining lymph nodes (aLNs) were excised and squeezed through a 70 µm cell strainer (352350, Corning). To isolate immune cells, the lungs and aortas in the thoracic cavities were removed after PBS perfusion and cut into small pieces, followed by a 30-minute digestion with type II (250 U/mL for lungs) or type I (150 U/mL for aortas) collagenase (LS004176/LS004196; Worthington Biochemical). Digested tissues and solutions were then mashed through a 70 µm cell strainer. Pulmonary leukocytes were further purified by a 40%/70% Percoll (17-0891-09; GE) gradient. In some experiments, splenic CD4$^+$, CD8$^+$ T cells or CD4$^+$CD62L$^+$CD44^{low} naive, CD4$^+$CD25$^-$ responder and CD4$^+$CD25$^+$ Treg cells were purified after staining with FITC/APC anti-mouse CD4 (100406/100412, 1:200), PERCP anti-mouse CD8a (100732, 1:200), PE anti-mouse CD25 (102007, 1:200), APC anti-mouse CD62L (104412, 1:200), Pacific Blue anti-mouse CD44 (103020, 1:200; all from Biolegend) via a FACSAria cell sorter (BD Biosciences). CD3$^+$ T cells, T-cell–depleted splenocytes, and CD11c$^+$ dendritic cells were obtained by using magnetic beads (480070/480078; Biolegend).

Real-Time Quantitative Polymerase Chain Reaction

Total RNA was extracted from purified CD3$^+$ T cells, T-cell–depleted splenocytes, in vitro–activated CD4$^+$ T cells, CD11c$^+$ dendritic cells, and thoracic aortas by the E.Z.N.A. HP Total RNA kit (R6812-02, OMEGA). cDNA was subsequently synthesized from 1 µg of RNA using Reverse Transcriptase M-MLV (2641A; TaKaRa) according to manufacturer's instructions. mRNA levels were quantitatively determined on an ABI StepOnePlus Sequence Detection System (Applied Biosystems) by SYBR-green technology. Polymerase chain reaction primers were designed (Table S1) and expressions of target genes were normalized to the average levels of the housekeeping genes RPS13 (ribosomal protein S13), HPRT (hypoxanthine phosphoribosyltransferase), GAPDH, and β-actin.

Cholesterol Efflux Assay

Labeling medium containing BODIPY-cholesterol (810255; Avanti Polar Lipids) was prepared by complexing the sterols (unlabeled cholesterol and BODIPY-cholesterol, 8:2) with CD (methyl-betta-cyclodextrin) at a molar ratio of 1:15 (cholesterol/CD; C3045/C4555; Sigma).[19] Purified CD4$^+$ and CD8$^+$ T cells from spleens of *Abca1*$^{CD4-/CD4-}$*Ldlr*$^{-/-}$ and control *Abca1*$^{+/+}$*Ldlr*$^{-/-}$ mice on NLD were labeled by incubation with 2.5 mM BODIPY-cholesterol-loaded CD in Iscove Modified Dulbecco Medium (31980030; Gibco) plus 0.2% fatty acid-free BSA (A8806; Sigma) and 2 µg/mL ACAT (Acyl CoA: cholesterol O-acyl transferases) inhibitor (S9318; Sigma) at 37 °C, 5% CO_2 for 60 minutes. After washing twice with fresh Iscove Modified Dulbecco Medium by a brief spin at 350*g* for 5 minutes, the cells were resuspended in Iscove Modified Dulbecco Medium for 1-hour equilibration. apo AI (10 µg/mL, 178452; Calbiochem) or HDL (50 µg/mL, YB-003; Yiyuan Biotechnologies) was then added into the cell suspension to initiate cholesterol efflux. Four hours later, efflux was stopped by a brief spin at 350*g* for 5 minutes to

remove the supernatant with acceptors. Samples treated without apo AI or HDL after equilibration was used as the baseline for efflux. Mean fluorescence intensity (MFI) of BODIPY-cholesterol on T cells was measured by flow cytometry (Calibur; BD Biosciences). The cholesterol efflux level was calculated as follows: (baseline MFI−remaining MFI)/baseline MFI×100.

Flow Cytometric Analyses

Cells were stained with antibodies against CD45, CD45.1, CD45.2, CD3, CD4, CD8, CD11b, CD11c, IA/IE, CD44, CD62L, CD28, CD137, CD27, OX40, CXCR3 (CXC motif chemokine receptor 3), CCR5 (CC motif chemokine receptor 5), or corresponding isotype controls (all from eBioscience or Biolegend), for 15 minutes at 4°C in PBS containing 1% normal C57BL/6J mouse serum. After washing, cells were subjected to flow cytometric analysis (Calibur; BD Biosciences) to determine the phenotype of T cells in different organs. The expressions of anti-apoptotic proteins Bcl-2 (B-cell lymphoma 2) and Bcl-xL (B-cell lymphoma extra-large) were determined by intracellular stainings with α-Bcl-2 (633509; Biolegend) and α-Bcl-xL (2764S; Cell Signaling Technology) antibodies. For assessment of IFN (interferon)-γ producing cells, cells were stimulated with PMA and ionomycin in the presence of brefeldin A (00-4975-93; eBioscience) for 16 hours before intracellular stainings with α-IFN-γ antibody (505810; Biolegend). Treg cells were visualized by intracellular stainings with α-Foxp3 antibody (12-5773-82, FJK-16s; eBioscience). IFN-γ and Foxp3-positive cells were identified using FMO (fluorescence minus one) controls. All antibodies were used at the dilution of 1:200 unless otherwise indicated.

For lipid raft analysis, cells were fixed in 4% polyformaldehyde at room temperature for 30 minutes immediately after cell surface staining. Cells were then incubated with biotin-labeled cholera toxin B subunit (C9972; Sigma) and PerCP-labeled streptavidin (405213; Biolegend) before analysis by flow cytometry.

To visualize TCR signaling, splenocytes were stimulated with 1 μg/mL α-CD3 antibody or 10 μg/mL $OVA_{323-339}$ peptide (RP10610; Genescript) for up to 90 minutes at 37°C, fixed with 4% paraformaldehyde and permeabilizated in ice-cold 100% methanol, followed by incubation with antibodies against surface markers and phosphorylated Zap70 (no. 2717, 1:800; α-Phospho-ZAP-70) and Erk (no. 4370, 1:800; α-Phospho-Erk1/2; both from Cell Signaling Technology).

Cell Culture and Functional Analysis

Fluorescence-activated cell sorting (FACS)–sorted splenic total $CD4^+$/$CD8^+$ T cells or $CD4^+CD62L^+CD44^{low}$ naive T cells were first labeled with CSFE (2.5 μM, C1157; Invitrogen), and then stimulated with plate-bound α-CD3 and soluble α-CD28 antibodies (both at 1 μg/mL, 100340/102116; Biolegend) for 24 or 72 hours. To determine the suppressive capacity of Treg cells, FACS-purified $CD4^+CD25^+$ Treg cells were cocultured with CSFE-labeled $CD4^+CD25^-$ responder T cells (1×10^5/well) at indicated ratios in the presence of soluble α-CD3 (2.5 μg/mL) and 2×10^5/well feeder cells (T-cell–depleted splenocytes) for 72 hours. The concentrations of IL (interleukin)-2 in supernatants after 24-hour culture were determined by ELISA (88-7024-88; eBioscience). Apoptotic cells were determined by 7-AAD and Annexin V (559763; BD Biosciences) stainings for 15 minutes at room temperature, and proliferation of (responder) T cells was visualized by CFSE profiles in flow cytometric analysis.

Adoptive Transfer Experiments

Purified $CD4^+CD62L^+CD44^{low}$ naive T cells (8×10^5/mice), from spleens of *CD4-Cre*$^+$*Abca1*$^{fl/fl}$OT-II or control *CD4-Cre*$^-$*Abca1*$^{fl/fl}$OT-II mice ($CD45.2^+$), were injected into the tail vein of untreated female $CD45.1^+$ recipients. Pilot experimental data (effect size 0.5, variability 0.2, significant level 0.05, power 0.9, and 1-sided test) were used to estimate the recipient sample size (n=4) using the online software (https://eda.nc3rs.org.uk/eda/login/auth). One day later, mice were intravenously immunized with 2 mg ovalbumin (LS0030054, OVA; Worthington) plus 20 μg lipopolysaccharide (L2880; Sigma). The phenotypes/numbers of donor-derived T cells in the blood, spleens, mesenteric lymph nodes, and lungs were analyzed/calculated by FACS on indicated days postimmunization. The expressions of IL-2 and IFN-γ in donor T cells were determined after restimulating splenocytes with 10 μg/mL $OVA_{323-339}$ peptide in the presence of brefeldin A (eBioscience) for 6 hours before intracellular stainings.

Statistical Analysis

The software Prism 8 (Graphpad, San Diego, CA) was used to generate graphs and perform statistics. Data were expressed as mean±SEM. To determine statistical significance for differences between 2 groups in experiments with $n<6$, a nonparametric Mann-Whitney *U* test was utilized. For $n\geq6$, normality was assessed with the Shapiro-Wilk test using $\alpha=0.05$, and the assumption of equal variances was analyzed using an *F* test. For all groups that passed these tests, unpaired *t* test was utilized. Mann-Whitney *U* test or unpaired *t* test with Welch correction were utilized for data that did not pass normality or *F* test, respectively. One-way ANOVA with Bonferroni multiple comparisons was used for data of >2 groups. Two-tailed calculations were used unless otherwise indicated. A level of $P<0.05$ was considered statistically significant.

RESULTS

Deletion of ABCA1 Markedly Inhibits T-Cell Cholesterol Efflux to Apo AI, but Slightly Reduces Membrane Contents of Cholesterol-Rich Lipid Rafts in T Cells

To investigate the role of *Abca1* in T cells and the importance of T-cell–specific ABCA1 in atherosclerosis, we used the *CD4-Cre* mouse strain to generate the conditional ABCA1 knockout mice (*Abca1*$^{CD4-/CD4-}$) on the *Ldlr*$^{-/-}$ background. The expression of CD4 in the $CD4^+CD8^+$ double-positive thymocytes triggers the expression of the Cre enzyme, which subsequently deletes the *Abca1* gene in these cells as well as the later mature $CD4^+$ and $CD8^+$ single-positive T cells in *Abca1*$^{CD4-/CD4-}$*Ldlr*$^{-/-}$ mice (Figure S1A). Indeed, the mRNA levels of ABCA1 were reduced >90% ($P<0.001$) in splenic $CD3^+$ T cells of *Abca1*$^{CD4-/CD4-}$*Ldlr*$^{-/-}$mice as compared to those of littermate *Abca1*$^{+/+}$*Ldlr*$^{-/-}$controls (Figure 1A). Of note, unlike macrophages with higher levels of ABCA1, T cells express

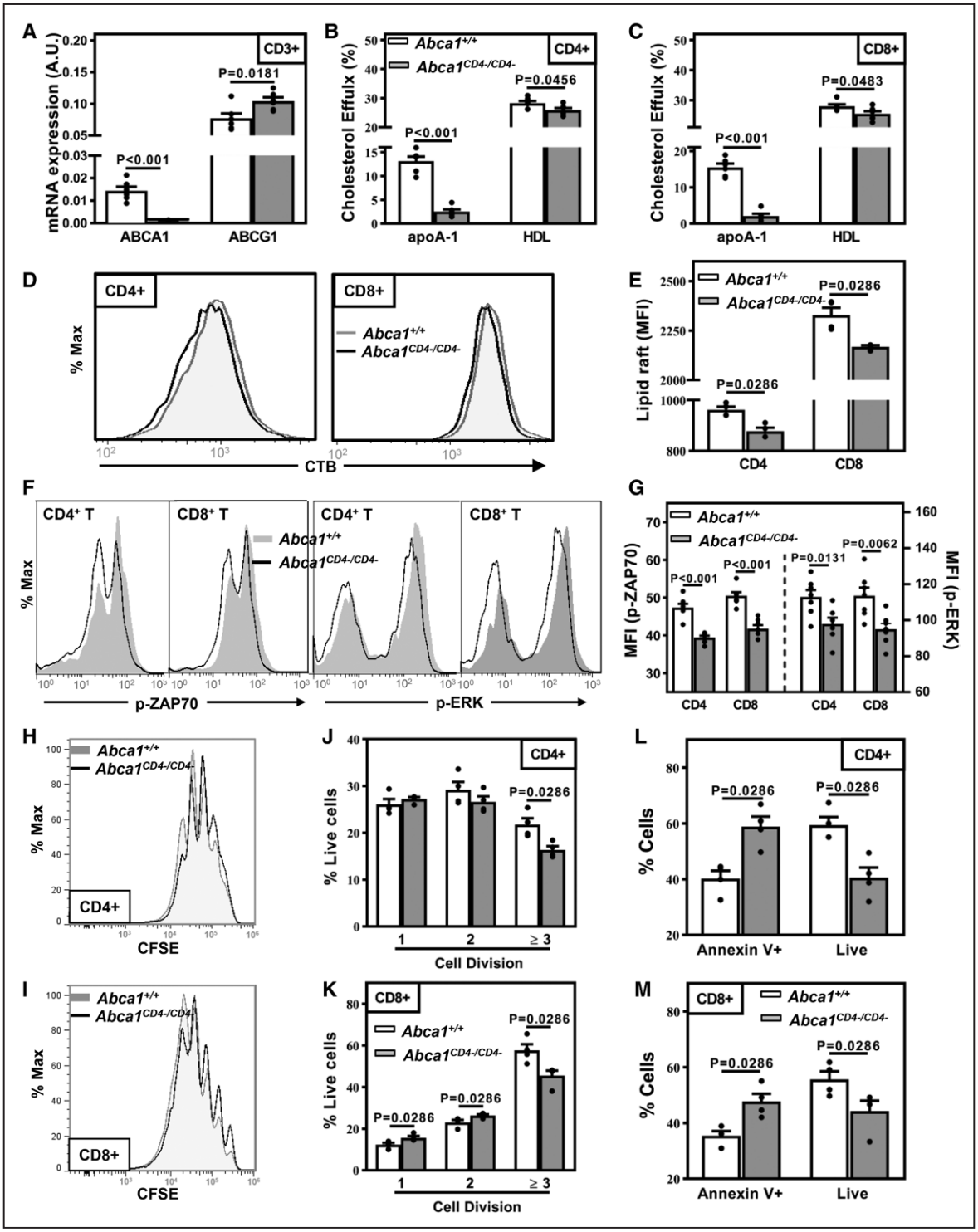

Figure 1. ABCA1 (ATP-binding cassette transporter A1) deletion inhibits T-cell proliferation and survival after activation in vitro. **A**, mRNA levels of ABCA1 and ABCG1 in purified CD3$^+$ T cells from female *Abca1*$^{CD4-/CD4-}$*Ldlr*$^{-/-}$ (gray bar) or littermate *Abca1*$^{+/+}$*Ldlr*$^{-/-}$ (open bar) mice (n=6 mice/group) on normal laboratory diet (NLD). **B** and **C**, Cellular cholesterol efflux to apo AI (10 μg/mL) or HDL (high-density lipoprotein; 50 μg/mL) from BODIPY-cholesterol loaded CD4$^+$ (**B**) or CD8$^+$ (**C**) T cells purified from female *Abca1*$^{CD4-/CD4-}$*Ldlr*$^{-/-}$ (gray bar) or control *Abca1*$^{+/+}$*Ldlr*$^{-/-}$ (open bar) mice (n=6 mice/group) on NLD. **D** and **E**, Representative histograms (**D**) or bar graphs (**E**) showing levels of lipid rafts, determined by CTB staining, on membranes of purified splenic CD4$^+$ or CD8$^+$ T cells from male *Abca1*$^{CD4-/CD4-}$*Ldlr*$^{-/-}$ (black line/gray bar) and *Abca1*$^{+/+}$*Ldlr*$^{-/-}$ (gray line/open bar) mice (n=4 mice/group) on NLD. **F** and **G**, Representative histograms (**F**) or bar graphs (**G**) showing the levels of phosphorylated ZAP70 (pZAP70) and ERK (pERK) in total CD4$^+$ or CD8$^+$ T cells from naive male *Abca1*$^{CD4-/CD4-}$*Ldlr*$^{-/-}$ versus *Abca1*$^{+/+}$*Ldlr*$^{-/-}$ mice (n=7 mice/group) upon activation. Cells were activated by soluble anti-CD3 (1 μg/mL) for 60 minutes before fixation/permeabilization and intracellular staining. **H–K**, Representative histograms showing the division of cells, illustrated by (*Continued*)

5-fold less ABCA1 than ABCG1 (Figure 1A). Interestingly, deletion of ABCA1 further upregulated the expression of ABCG1 in T cells at both mRNA (1.32-fold, P=0.0181; Figure 1A) and protein (1.81-fold, P=0.0286; Figure S1B and S1C) levels. As expected, expressions of ABCA1 and ABCG1 in non-CD3$^+$ (ie, T cell–depleted) splenocytes and liver tissues were not affected in *Abca1*$^{CD4-/CD4-}$*Ldlr*$^{-/-}$mice (Figure S1D and S1E), corroborating the T-cell–specific depletion of ABCA1 in these mice.

Deletion of ABCA1 dramatically inhibited apo AI–mediated cholesterol efflux from both CD4$^+$ (0.19-fold, P<0.001) and CD8$^+$ (0.14-fold, P<0.001) T cells (Figure 1B and 1C). Moreover, despite the upregulation of ABCG1, ABCA1$^{-/-}$ T cells showed slight reductions (≈9%) in cholesterol efflux to HDL (Figure 1B and 1C), likely due to the absence of cholesterol transport from T cells via ABCA1 to small dense HDL.[20] As expected, no differences in cholesterol efflux to apo AI were observed in macrophages isolated from control versus *Abca1*$^{CD4-/CD4-}$*Ldlr*$^{-/-}$mice (Figure S1F). Cholesterol is an important component of membrane lipid rafts, and the membrane contents of lipid raft can be quantified using fluorescently-labeled CT-B (cholera toxin B), which binds to the pentasaccharide chain of ganglioside GM1, a raft-associated lipid.[17] Interestingly, no increment of membrane lipid rafts was detected in ABCA1-deficient splenic T cells that had impaired cholesterol efflux capacities. Instead, a slight but significant decrease of membrane lipid rafts was observed on both ABCA1$^{-/-}$ CD4$^+$ (0.91-fold, P=0.0286) and CD8$^+$ (0.93-fold, P=0.0286) T cells as compared to the corresponding control (*Abca1*$^{+/+}$) T cells (Figure 1D and 1E). Thus, specific knockout of ABCA1 in T cells markedly inhibits the cholesterol efflux to apo AI, but slightly reduces the contents of lipid raft in the cell membrane.

ABCA1-Deficient T Cells Display Impaired TCR Signaling, Reduced Proliferation, and Increased Apoptosis After Activation In Vitro

Next, we compared the development and phenotype of T cells between *Abca1*$^{CD4-/CD4-}$*Ldlr*$^{-/-}$ and *Abca1*$^{+/+}$*Ldlr*$^{-/-}$mice on NLD. The thymic weights and cellularities were comparable between these 2 groups of mice (Figure S2A). In the thymus, T cell precursors immigrated from the bone marrow undergo a step-wise differentiation from CD4$^-$CD8$^-$ double-negative to the CD4$^+$CD8$^+$ CD4$^+$CD8$^+$ double-positive stage before diverging into either CD4$^+$CD8$^-$ or CD4$^-$CD8$^+$ single-positive T cells that eventually migrate into the periphery. The percentages of thymic CD4$^+$ and CD8$^+$ single-positive as well as CD4$^+$CD8$^+$ double-positive T cells were comparable between *Abca1*$^{CD4-/CD4-}$*Ldlr*$^{-/-}$ and *Abca1*$^{+/+}$*Ldlr*$^{-/-}$mice, showing that deletion of ABCA1 in CD4$^+$CD8$^+$ double-positive thymocytes has no impact on their further development into CD4/8 single-positive T cells in the thymus (Figure S2B).

In the periphery, the absolute numbers of splenocytes as well as splenic CD4$^+$ and CD8$^+$ T cells did not differ significantly between control and *Abca1*$^{CD4-/CD4-}$*Ldlr*$^{-/-}$mice (Figure S2C). Based on expressions of CD44 and CD62L, mature T cells can be subdivided into the following four subsets: naive (CD44$^-$CD62L$^+$), central memory (CD44$^+$CD62L$^+$), EM (CD44$^+$CD62L$^-$) and effector (CD44$^-$CD62L$^-$) T cells. Frequencies of these 4 subsets in both CD4$^+$ and CD8$^+$ T-cell compartments were comparable between control and T-cell specific ABCA1-deficient mice as well (Figure S2D and S2E). Thus, T-cell–intrinsic ABCA1 has little impact on the number and phenotype of peripheral T cells under homeostatic conditions in vivo.

Given the importance of lipid rafts in signaling transduction, we further explored the roles of ABCA1 on TCR signaling and TCR-driven T-cell proliferation. The deletion of ABCA1 did not alter the basal expressions of TCR and CD3 on splenic CD4$^+$ or CD8$^+$ T cells in mice (data not shown). However, upon activation by anti-CD3, the phosphorylation of both ZAP (pZAP70) and ERK (pERK), 2 important molecules along the TCR signaling pathway, were considerably reduced by ≈20% in ABCA1$^{-/-}$ CD4$^+$ and CD8$^+$ T cells in comparison to those in ABCA1-sufficient counterparts (Figure 1F and 1G). Accordingly, ABCA1$^{-/-}$ CD4$^+$ and CD8$^+$ T cells showed a ≈25% reduction in capacities to divide three or more times after TCR stimulation, accompanied by a concomitant ≈35% increase of apoptotic cells (Figure 1H through 1M).

Taken together, despite little impact on in vivo developing thymocytes and the number/phenotype of mature T cells in the periphery under homeostatic conditions, deficiency of ABCA1 impairs TCR signaling, inhibits the proliferation while promotes apoptosis of T cells upon activation in vitro.

T-Cell–Specific Deletion of ABCA1 Reduces Arterial Accumulations of T Cells, and Ameliorates the Development of Atherosclerosis in Ldlr$^{-/-}$ Mice on WTD

To induce the formation of atherosclerosis, *Abca1*$^{CD4-/CD4-}$*Ldlr*$^{-/-}$ and littermate *Abca1*$^{+/+}$*Ldlr*$^{-/-}$ control mice were fed a high fat/cholesterol WTD for 9 weeks. WTD

Figure 1 Continued. CFSE dilutions (**H** and **I**), or mean percents of divided cells (**J** and **K**) of CD4$^+$ (**H** and **J**) or CD8$^+$ (**I** and **K**) T cells isolated from male *Abca1*$^{CD4-/CD4-}$*Ldlr*$^{-/-}$ (black line/gray bar) and *Abca1*$^{+/+}$*Ldlr*$^{-/-}$ (gray line/open bar) mice on NLD (n=4 mice/group). **L** and **M**, Activation-induced apoptosis of CD4$^+$ (**L**) or CD8$^+$ (**M**) T cells isolated from male *Abca1*$^{CD4-/CD4-}$*Ldlr*$^{-/-}$ (gray bar) and *Abca1*$^{+/+}$*Ldlr*$^{-/-}$ (open bar) mice on NLD (n=4 mice/group). CSFE-labeled (**H**–**K**) or nonlabeled (**L** and **M**) CD4$^+$/CD8$^+$ T cells were stimulated with 1 μg/mL plate-bound α-CD3 plus soluble α-CD28 antibodies. CSFE dilutions and cellular apoptosis were determined by fluorescence-activated cell sorting (FACS) after 72 hours of activation. Data are expressed as mean±SEM. Results in **A**–**C** and **G** were compared with unpaired *t* test, and results in **E** and **J**–**M** were compared with unpaired Mann-Whitney *U* test. A.U. indicates arbitrary unit; CTB, cholera toxin B; and MFI, mean fluorescence intensity.

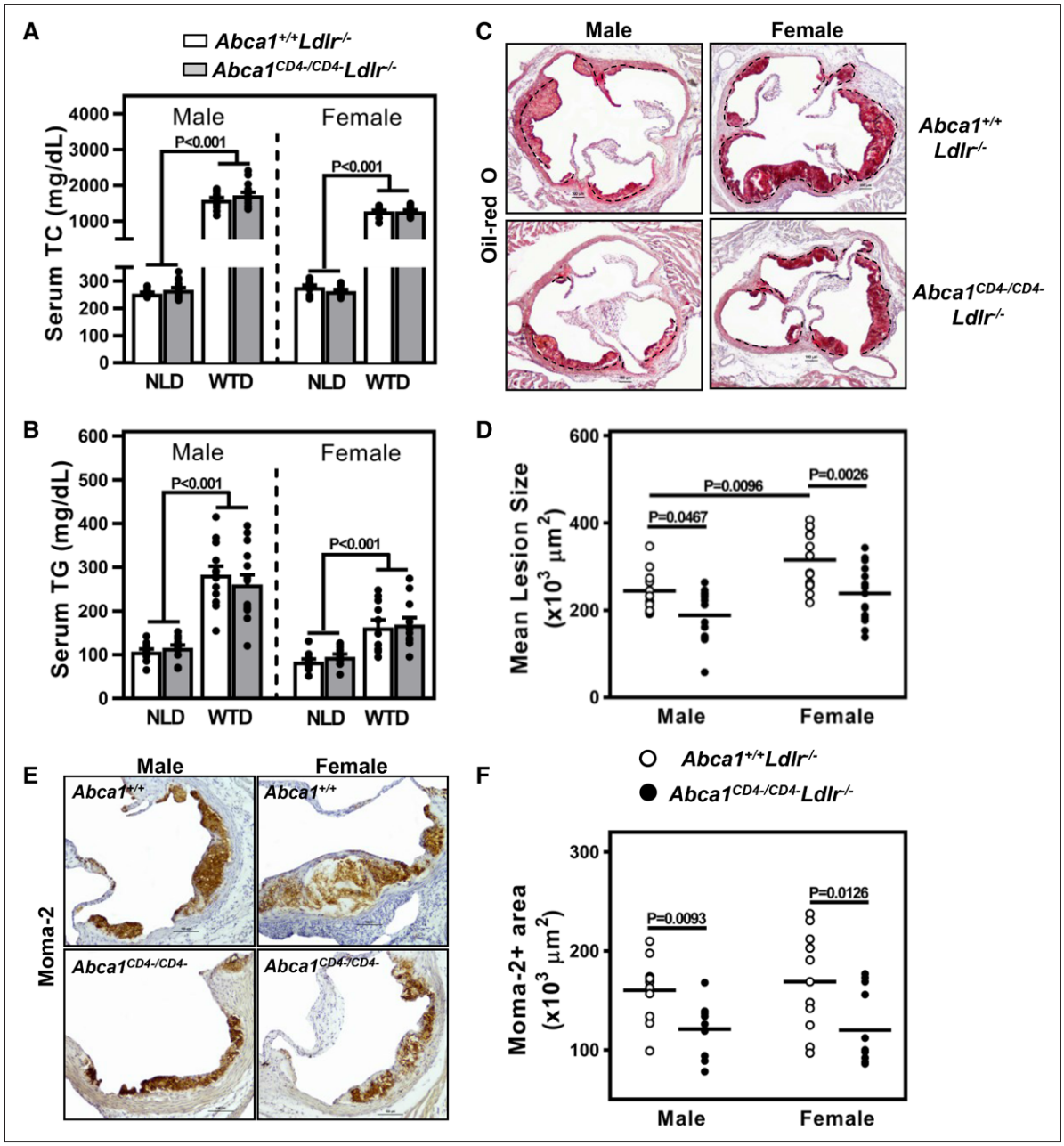

Figure 2. T-cell–specific deletion of ABCA1 (ATP-binding cassette transporter A1) ameliorates the development of atherosclerosis in Ldlr$^{-/-}$ mice on Western-type diet (WTD).

Animals were fed with WTD for 9 weeks to induce the formation of atherosclerotic lesions. **A** and **B**, Plasma total cholesterol (TC; **A**) and triglyceride (TG; **B**) levels of *Abca1*$^{CD4-/CD4-}$*Ldlr*$^{-/-}$ (gray bar) and *Abca1*$^{+/+}$*Ldlr*$^{-/-}$ (open bar) mice on normal laboratory diet (NLD) or WTD (n=13–16 mice/group). **C** and **D**, Representative photomicrographs showing oil-red-O stained sections (original magnification 4×10) with dashed lines to mark the border of atherosclerotic lesions (**C**) and mean atherosclerotic lesion sizes at aortic roots (**D**). **E** and **F**, Representative photomicrographs showing α-Moma-2 stained sections (brown, 10x10) counterstained by hematoxylin (**E**), and mean absolute macrophage contents (**F**) in aortic roots of *Abca1*$^{CD4-/CD4-}$*Ldlr*$^{-/-}$ (black dot) and *Abca1*$^{+/+}$*Ldlr*$^{-/-}$ (open dot) mice. Each symbol represents the mean lesion area in a single mouse and the horizontal line indicates the mean of the group. Results in **A**, **B**, and **D** were analyzed with one-way ANOVA with Bonferroni multiple comparisons. Results in **F** were compared with unpaired *t* test (*P*=0.0093, male) or Mann-Whitney *U* test (*P*=0.0126, female).

feeding significantly increased plasma total cholesterol and triglyceride levels in both animal groups, but no effects of T-cell ABCA1 deletion on serum total cholesterol and triglyceride levels were observed in either male or female mice (Figure 2A and 2B). Moreover, female *Abca1*$^{+/+}$*Ldlr*$^{-/-}$animals developed considerably larger lesions (1.29-fold, *P*=0.0096) at aortic roots than the male counterparts. Nonetheless, the lesion size in *Abca1*$^{CD4-/CD4-}$*Ldlr*$^{-/-}$ mice, irrespective of the gender, was significantly smaller (male: 0.79-fold, *P*=0.0467; female: 0.76-fold, *P*=0.0026) than that in *Abca1*$^{+/+}$*Ldlr*$^{-/-}$controls (Figure 2C and 2D).

IHC stainings demonstrated that lesions at the aortic roots were mainly composed of Moma-2 positive

macrophages (Figure 2E). Despite no effects on the relative macrophage contents (Figure S3A and S3B), T-cell specific deletion of ABCA1 significantly reduced the absolute amounts of macrophages in atherosclerotic lesions in both males (0.75-fold, P=0.0093) and females (0.71-fold, P=0.0126; Figure 2F), likely owing to the reduced lesion sizes in these mice (Figure S3A and S3B). In female *Abca1*$^{CD4-/CD4-}$*Ldlr*$^{-/-}$animals, the relative contents of necrotic cores were also reduced (0.40-fold, P=0.0121, data not shown), whereas this was not observed in male animals due to the absence of visible necrotic cores in both genotypes.

Strikingly, a ≈50% reduction of CD3$^+$ T cells was noted in lesions and the surrounding adventitias in *Abca1*$^{CD4-/CD4-}$*Ldlr*$^{-/-}$ mice, regardless of the genders, compared to that in corresponding *Abca1*$^{+/+}$*Ldlr*$^{-/-}$controls (Figure 3A and 3B). Given that the formation of lesions in the aortic arch is much slower than that at the aortic roots in mice on *LDLr*$^{-/-}$ background, we further analyzed the number of CD4$^+$/CD8$^+$ T cells in aortic arch of female mice with larger lesions and more T cells. As expected, female *Abca1*$^{CD4-/CD4-}$*Ldlr*$^{-/-}$ mice also had significantly reduced numbers of both CD4$^+$ and CD8$^+$ T cells in thoracic aortas (CD4$^+$: 0.49-fold, P=0.0362; CD8$^+$: 0.54-fold, P=0.0326 versus *Abca1*$^{+/+}$*Ldlr*$^{-/-}$controls; Figure 3C), although the percentages of CD3$^+$CD11b$^-$ T cells among gated CD45$^+$ leukocytes and the ratio of CD4$^+$/CD8$^+$ T cells within gated CD3$^+$CD11b$^-$ compartment were comparable (data not shown). Notably, a highly positive correlation was witnessed between the numbers of CD4$^+$ and CD8$^+$ T cells in aortas (Figure 3C). At the mRNA level, similar reductions and correlations of CD4 and CD8 expressions were also observed in thoracic aortas of female *Abca1*$^{CD4-/CD4-}$*Ldlr*$^{-/-}$ mice (Figure 3D).

In sum, specific deletion of ABCA1 in T cells alleviates atherogenesis in *Ldlr*$^{-/-}$ mice, which is associated with reduced arterial accumulations of T cells.

ABCA1 Deficiency Alters the Phenotype and Function of T Cells in WTD-Fed *Ldlr*$^{-/-}$ Mice

Akin to situations in naive mice, the development of thymocytes and absolute numbers of CD4$^+$ and CD8$^+$ T cells in spleens, blood, lungs, and aortic lymph nodes were comparable between control and *Abca1*$^{CD4-/CD4-}$*Ldlr*$^{-/-}$ mice after 9-week WTD feeding (Figure S4A through S4F), ruling out the possibility that less T cells in lesions were simply attributed to a general T-cell deficiency in *Abca1*$^{CD4-/CD4-}$*Ldlr*$^{/}$ mice on WTD. However, upon WTD challenge, surface levels of TCR decreased slightly (≈10%) on ABCA1-deficient CD4$^+$ and CD8$^+$ T cells in spleens (P<0.001/P<0.001) and aortic lymph nodes (P=0.0038/0.0022; data not shown), which may further attenuate TCR signaling and alter the phenotypes of peripheral T cells.

We thus speculated that reduced migration/infiltration or increased apoptosis of T cells may underlie the phenomena (described in Figure 3) in atherosclerotic *Abca1*$^{CD4-/CD4-}$*Ldlr*$^{-/-}$ mice. To test these hypotheses, we first compared the expressions of a panel of chemokine receptors and anti/proapoptotic genes in in vitro–activated control versus ABCA1-deleted splenic CD4$^+$ T cells by quantitative polymerase chain reaction or FACS analyses. Significant reductions in mRNA levels of CCR5 (≈25%) and CXCR3 (≈45%) were detected in ABCA1$^{-/-}$ CD4$^+$ T cells early (24 hours) after activation (Figure 4A), whereas their CCR1 and CCR2 levels were comparable to those in control cells (data not shown). Accordingly, the surface protein levels of both CCR5 and CXCR3 on ABCA1$^{-/-}$ CD4$^+$ T cells were reduced by ≈20% at 72 hours poststimulation (Figure 4A). Moreover, expressions of the antiapoptotic proteins Bcl-2 and Bcl-xL but not the proapoptotic molecules BIM, BAX and BAK, were significantly lower at both the mRNA (≈50%) and protein (≈25%) levels in ABCA1$^{-/-}$ CD4$^+$ T cells (Figure 4B and 4C). In accordance with the above in vitro findings, frequencies of CD4$^+$ and CD8$^+$ T cells expressing CCR5 were significantly decreased in spleens (≈25%), blood (≈30%), lungs (≈35%) and aLNs (≈20%) of *Abca1*$^{CD4-/CD4-}$*Ldlr*$^{-/-}$ mice than those in control *Abca1*$^{+/+}$*Ldlr*$^{-/-}$ mice after 9-week WTD feeding (Figure 4D through 4G). Similar reductions in percentages of CXCR3 positive CD4$^+$ T cells were also observed in all organs analyzed in *Abca1*$^{CD4-/CD4-}$*Ldlr*$^{-/-}$ mice, whereas percents of CXCR3-expressing CD8$^+$ T cells were mildly decreased in lymphatic organs (≈10%) and lungs (≈25%) as well (Figure 4D through 4G). Furthermore, splenic CD4$^+$ and CD8$^+$ T cells in WTD-fed *Abca1*$^{CD4-/CD4-}$*Ldlr*$^{-/-}$ mice expressed significantly less antiapoptotic proteins Bcl-2 (≈30%) and Bcl-xL (≈20%; Figure 4H). Together, these data indicated that ABCA1 promotes the migration/infiltration and survival of activated T cells by upregulating CCR5/CXCR3 and Bcl-2/Bcl-xL, respectively, in atherosclerotic-prone arteries.

In addition, ABCA1$^{-/-}$ CD4$^+$ T cells expressed ≈70% less IFN-γ at both mRNA and protein levels upon TCR activation in vitro (Figure 4I). Likewise, significantly reduced percentages of IFN-γ–positive CD4$^+$ and CD8$^+$ T cells were observed in both spleens (≈25%) and aLNs (≈30%) of WTD-fed *Abca1*$^{CD4-/CD4-}$*Ldlr*$^{-/-}$ mice (Figure 4J and 4K). An approximate 40% reduction (P=0.0251) in mRNA levels of IFN-γ were also noted in thoracic aortas of *Abca1*$^{CD4-/CD4-}$*Ldlr*$^{-/-}$ mice as well (data not shown).

Collectively, depletions of ABCA1 in T cells lead to reduced surface CCR5/CXCR3 expressions, decreased antiapoptotic proteins Bcl-2 and Bcl-xL, and hampered IFN-γ–producing abilities of activated T cells in mice on WTD, all of which may contribute to the significant decline of T cell numbers in lesions and the amelioration of atherosclerosis development

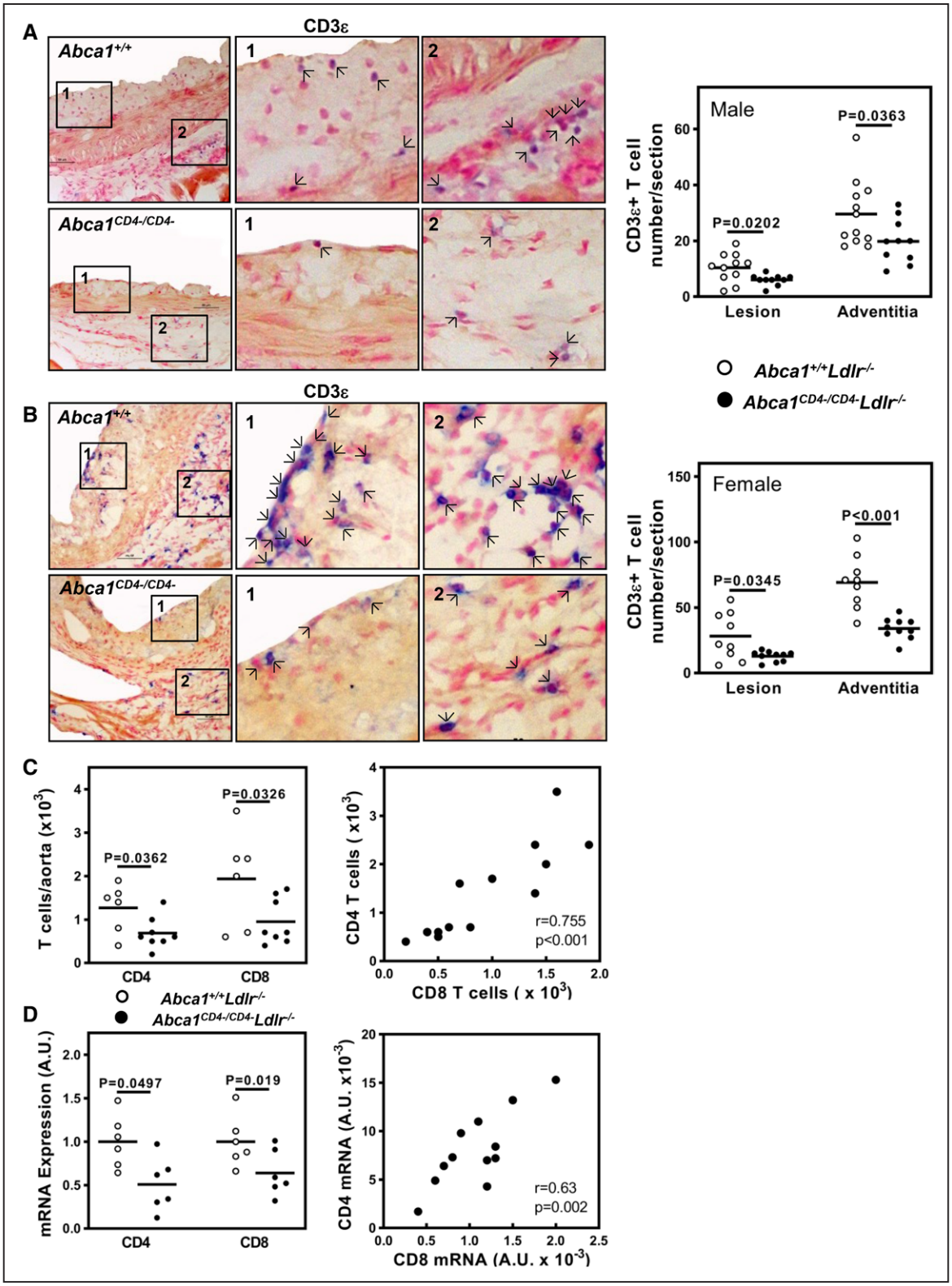

Figure 3. Significantly reduced T-cell accumulations in atherosclerotic lesions of T-cell–specific ABCA1- (ATP-binding cassette transporter A1) deficient mice on Western-type diet.

A and **B**, Representative photomicrographs showing α-CD3 stained sections (blue, indicated by arrows, ×400), counterstained by fast nuclear red (**left**), and mean numbers of CD3⁺ T cells (**right**) in atherosclerotic lesions and surrounding adventitias of male (**A**) or female (**B**) *Abca1*$^{CD4-/CD4-}$*Ldlr*$^{-/-}$ (black dot) and *Abca1*$^{+/+}$*Ldlr*$^{-/-}$ (open dot) mice. **C** and **D**, Numbers of CD4⁺/CD8⁺ T cells (**C**) or mRNA expressions of CD4/CD8 (**D**) in thoracic aorts of female *Abca1*$^{CD4-/CD4-}$*Ldlr*$^{-/-}$ (black dot) and *Abca1*$^{+/+}$*Ldlr*$^{-/-}$ (open dot) mice (**left**) and their correlation (**right**). Each symbol represents the mean value in a single mouse and the horizontal line indicates the mean of the group. All results were compared with unpaired *t* test. *P* values in **A** (0.0202, lesion) and **B** were corrected with Welch test. A.U. indicates arbitrary unit.

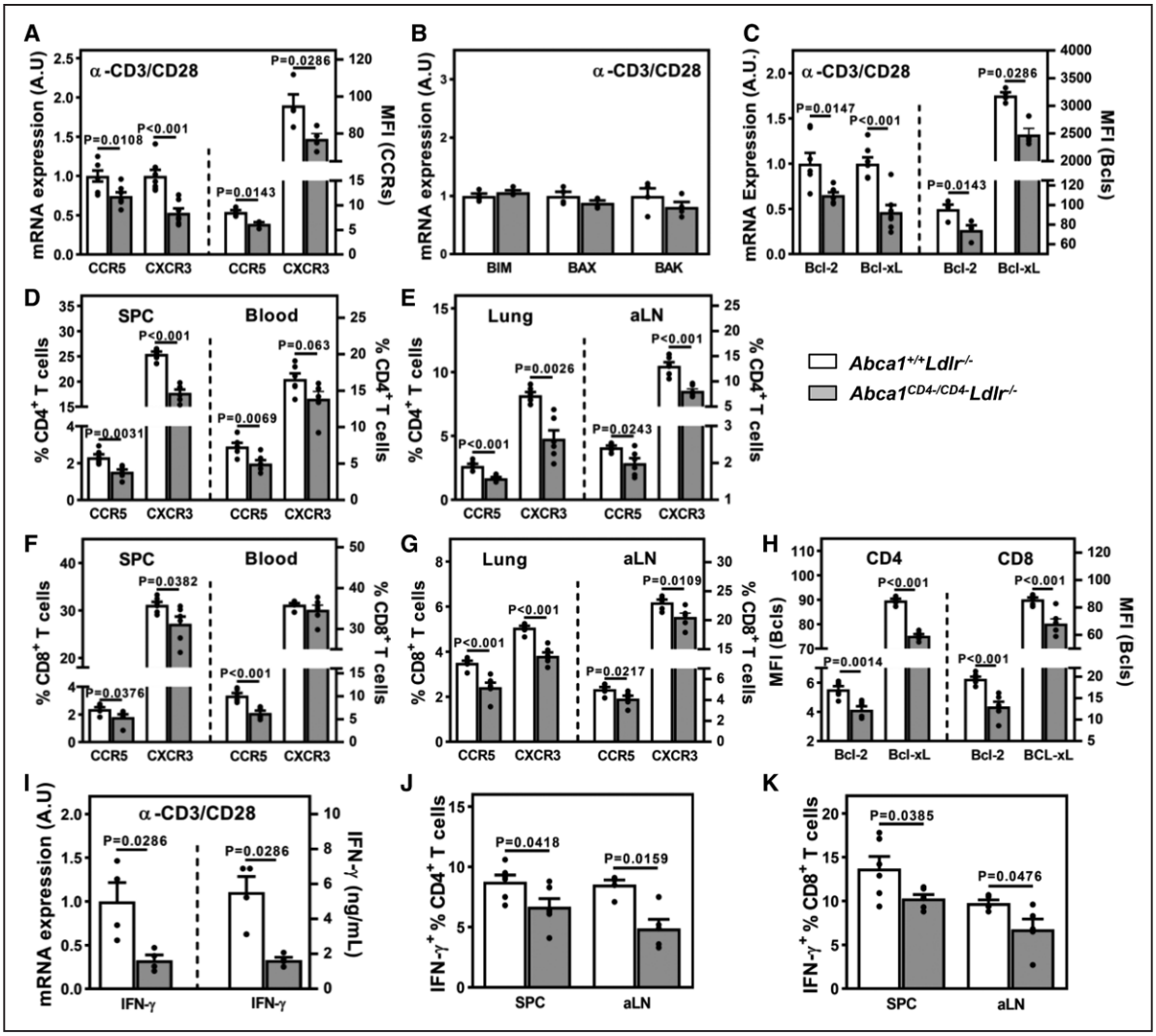

Figure 4. Deletion of ABCA1 (ATP-binding cassette transporter A1) reduces the expressions of chemokine receptors and antiapoptotic proteins, and hampers the effector functions of T cells both in vitro and in vivo.
A–**C**, Expressions of indicated chemokine receptors (**A**), proapoptotic (**B**) or antiapoptotic (**C**) proteins on/in activated CD4+ T cells. Purified splenic CD4+ T cells, from naive female *Abca1*$^{CD4-/CD4-}$*Ldlr*$^{-/-}$ or control *Abca1*$^{+/+}$*Ldlr*$^{-/-}$ mice, were stimulated with plate-bound α-CD3 and soluble α-CD28 (both at 1 μg/mL) for 24/72 hours before RNA extraction/fluorescence-activated cell sorting (FACS) analysis, respectively. Expressions were determined by quantitative polymerase chain reaction (Q-PCR; n=7 mice/genotype) or FACS (n=4 mice/genotype). **D**–**G**, Percentages of CCR5+ (CC motif chemokine receptor 5) or CXCR3+ (CXC motif chemokine receptor 3) cells within gated CD4+ (**D** and **E**) or CD8+ (**F** and **G**) T cell compartment in indicated tissues of female *Abca1*$^{CD4-/CD4-}$*Ldlr*$^{-/-}$ versus *Abca1*$^{+/+}$*Ldlr*$^{-/-}$ mice after 9-week Western-type diet (WTD) feeding (n=6 mice/group). **H**, Expressions of antiapoptotic Bcl-2 (B-cell lymphoma 2) and Bcl-xL (B-cell lymphoma extra-large), determined by FACS, in splenic CD4+ and CD8+ T cells in WTD-fed female *Abca1*$^{CD4-/CD4-}$*Ldlr*$^{-/-}$ versus *Abca1*$^{+/+}$*Ldlr*$^{-/-}$ mice (n=6 mice/group). **I**, Levels of IFN (interferon)-γ in activated CD4+ T cells or culture supernatants. CD4+ T cells, purified from spleens of female *Abca1*$^{CD4-/CD4-}$*Ldlr*$^{-/-}$ or control *Abca1*$^{+/+}$*Ldlr*$^{-/-}$ mice on normal laboratory diet, were activated with anti-CD3/28 in vitro. Expressions of IFN-γ in cells/culture supernatants were analyzed by Q-PCR (24 hours)/ELISA (72 hours), respectively (n=4 mice/group). **J** and **K**, Percentages of IFN-γ+ cells within gated CD4+ (**J**) or CD8+ (**K**) T cells in spleens (SPC) or aortic lymph nodes (aLN) of WTD-fed female mice (n=5–6 mice/group). Data are expressed as mean±SEM. mRNA and mean fluorescence intensity (MFI) results in **A**–**C** were compared with unpaired *t* test and Mann-Whitney *U* test, respectively. Results in **D**–**H** and **J**–**K** (SPC) were compared with unpaired *t* test, and *P* values (0.0026 and 0.0243) in **E** were corrected with Welch test. Results in **I**–**K** (aLN) were compared with unpaired Mann-Whitney *U* test. A.U. indicates arbitrary unit.

in *Abca1*$^{CD4-/CD4-}$*Ldlr*$^{-/-}$ mice. Of note, it is unlikely that these aberrant phenotypes and functions of activated ABCA1-deficient T cells are related to impaired costimulatory signaling, as expressions of many costimulatory molecules were unaltered or even slightly increased in *Abca1*$^{CD4-/CD4-}$*Ldlr*$^{-/-}$ mice on NLD or WTD (Figure S4G through S4J).

T-Cell–Specific Deletion of ABCA1 Reduces the Frequency of EM T Cells During the Development of Atherosclerosis

Interestingly, detailed phenotypic analyses revealed a slight but consistent increase of naive T cells at the expense of EM T cells in both splenic CD4+ (NA:

1.22-fold, P=0.026; EM: 0.80-fold, P=0.0152) and CD8$^+$ (NA: 1.10-fold, P=0.0368; EM: 0.71-fold, P=0.0022) T-cell compartments in female *Abca1*$^{CD4-/CD4-}$*Ldlr*$^{-/-}$mice on WTD (Figure 5A and 5B). A similarly altered T-cell phenotype was observed in T-cell ABCA1 deficient male animals on WTD as well (data not shown). Because EM T cells preferentially reside in extralymphoid tissues,[21] the decreased numbers of splenic EM T cells in *Abca1*$^{CD4-/CD4-}$*Ldlr*$^{-/-}$mice may result from an increased egress of these cells into other tissues, for instance, lungs. We thus analyzed the phenotype of T cells in the circulation and lungs of these two groups of mice after WTD feeding. Although the percentages of EM T cells in lungs were significantly higher than those in the blood and spleens as expected, similar declines of EM T cells as observed in spleens, were evident in the circulation (≈20%) and lungs (≈25%) of *Abca1*$^{CD4-/CD4-}$*Ldlr*$^{-/-}$mice (Figure 5C through 5F). Therefore, it is unlikely that the decreased numbers of EM T cells in lymphatic organs of *Abca1*$^{CD4-/CD4-}$*Ldlr*$^{-/-}$mice after WTD feeding can be attributed to their altered distributions among different tissues. Furthermore, the percentages of EM T cells were also decreased in aLNs (CD4$^+$: 0.76-fold, P=0.0317; CD8$^+$: 0.79-fold, P=0.0397) of mice with T cell–targeted deletion of ABCA1 (Figure 5G and 5H).

Notably, the number and suppressive function of Foxp3$^+$ Treg cells were comparable in spleens and aLNs of these two groups of mice (Figure S5A through S5C). Moreover, the expressions of Foxp3 in aortas of *Abca1*$^{CD4-/CD4-}$*Ldlr*$^{-/-}$mice tended to decrease by ≈50% (P=0.08) after normalization to CD4 (data not shown). Together, these data indicate that the reduced numbers of EM T cells and decreased arterial accumulation of T cells in *Abca1*$^{CD4-/CD4-}$*Ldlr*$^{-/-}$mice on WTD were not the consequence of augmented suppressions conferred by Treg cells in vivo.

ABCA1 Deficiency Reduces the Generation, Survival, and Function of CD4$^+$ Memory T Cells In Vivo

Given the weak expression of CD4 on dendritic cells, it is possible that the profound defects of EM T cells in WTD-fed *Abca1*$^{CD4-/CD4-}$*Ldlr*$^{-/-}$ mice may partially stem from the altered dendritic cells with reduced ABCA1 expressions. However, no differences in the number of dendritic cells and their expressions of ABCA1 and MHC-II were observed in *Abca1*$^{CD4-/CD4-}$*Ldlr*$^{-/-}$ versus control mice (Figure S5D and S5E).

Next, we isolated CD4$^+$CD44$^-$CD62L$^+$ naive T cells and subsequently stimulated them with α-CD3 and α-CD28 in vitro to explore T-cell–intrinsic roles of ABCA1 in the generation/maintenance of EM T cells. The activation of CD4$^+$ naive T cells was suppressed by the deletion of ABCA1 as evidenced by reduced expression of CD25 on cell surface (0.93-fold, P=0.026) and IL-2 levels in supernatants (0.91-fold, P=0.0079) early (24 hours) after stimulation (Figure 6A). Notably, similar to our in vivo findings depicted in Figure 5, ABCA1 deficiency resulted in significantly reduced numbers of CD44^{++} memory T cells at 72 hours post stimulation (0.89-fold, P=0.0065; Figure 6B). Considering the reduced IL-2 and CD25 expressions in ABCA1-depleted T cells upon activation (Figure 6A), and the importance of IL-2/CD25 signaling in T-cell survival,[22] we reasoned that the reduced amounts of CD44^{++} memory ABCA1-deficient T cells in vitro may be attributed to the increased apoptosis of these cells. We thus sorted CD44^{++}CD4$^+$ memory T cells generated in vitro (72 hours) and analyzed their cellular viabilities/apoptosis upon further culture. Indeed, significantly more apoptotic cells were observed in cultured ABCA1-deficient CD44^{++}CD4$^+$ memory T cells (1.3-fold, P=0.0317) compared with those in ABCA1$^{+/+}$ control counterparts on day 3 (Figure 6C), and this difference was almost completely abrogated by addition of exogenous IL-2 (Figure 6D). Hence, it appears that deletion of ABCA1 promotes the apoptosis of memory CD4$^+$ T cells mainly via repressing IL-2/CD25 signaling. Importantly, the in vitro survival of EM, but not naive, CD4$^+$ T cells sorted from spleens of *Abca1*$^{CD4-/CD4-}$*Ldlr*$^{-/-}$ mice on NLD, were significantly decreased (0.84-fold, P=0.0286) as well (Figure 6E).

To further confirm the T-cell–intrinsic roles of ABCA1 in memory T cells in vivo, naive CD4$^+$ OT-II T cells, purified from spleens of *Abca1*$^{CD4-/CD4-}$OT-II or *Abca1*$^{+/+}$OT-II mice (CD45.2$^+$), were intravenously administered into CD45.1$^+$ congenic recipients, which were challenged with OVA and lipopolysaccharide 24 hours later as described previously.[21] As expected, the TCR signaling of these ABCA1$^{-/-}$ T cells was impaired upon stimulation with cognate peptide in vitro as well (data not shown). On day 4 post immunization, significantly less (0.68-fold, P=0.0143) donor-derived CD45.2$^+$ABCA1$^{-/-}$ T cells, compared with CD45.2$^+$ABCA1$^{+/+}$ controls, were detected in the circulation of CD45.1$^+$ recipients (Figure 6F). With the cessation of antigen-induced proliferation in vivo, most antigen-specific T cells die while a minority of them survive and differentiate into memory T cells.[23] In accordance with our in vitro data, numbers of ABCA1$^{-/-}$ donor-derived CD4$^+$ memory T cells were significantly reduced in the blood (0.44-fold, P=0.0143), spleens (0.42-fold, P=0.0286), mesenteric lymph nodes (0.29-fold, P=0.0286) and lungs (0.55-fold, P=0.0429) of recipients 14 days after OVA inoculation (Figure 6F and 6G). In addition, these ABCA1$^{-/-}$ memory T cells, generated in vivo, produced profoundly less IL-2 (0.38-fold, P=0.0286) and IFN-γ (0.63-fold, P=0.0286) upon restimulation via TCR in vitro (Figure 6H).

Thus, deletion of ABCA1 suppresses the formation and function of memory CD4$^+$ T cells in a cell-intrinsic manner both in vitro and in vivo.

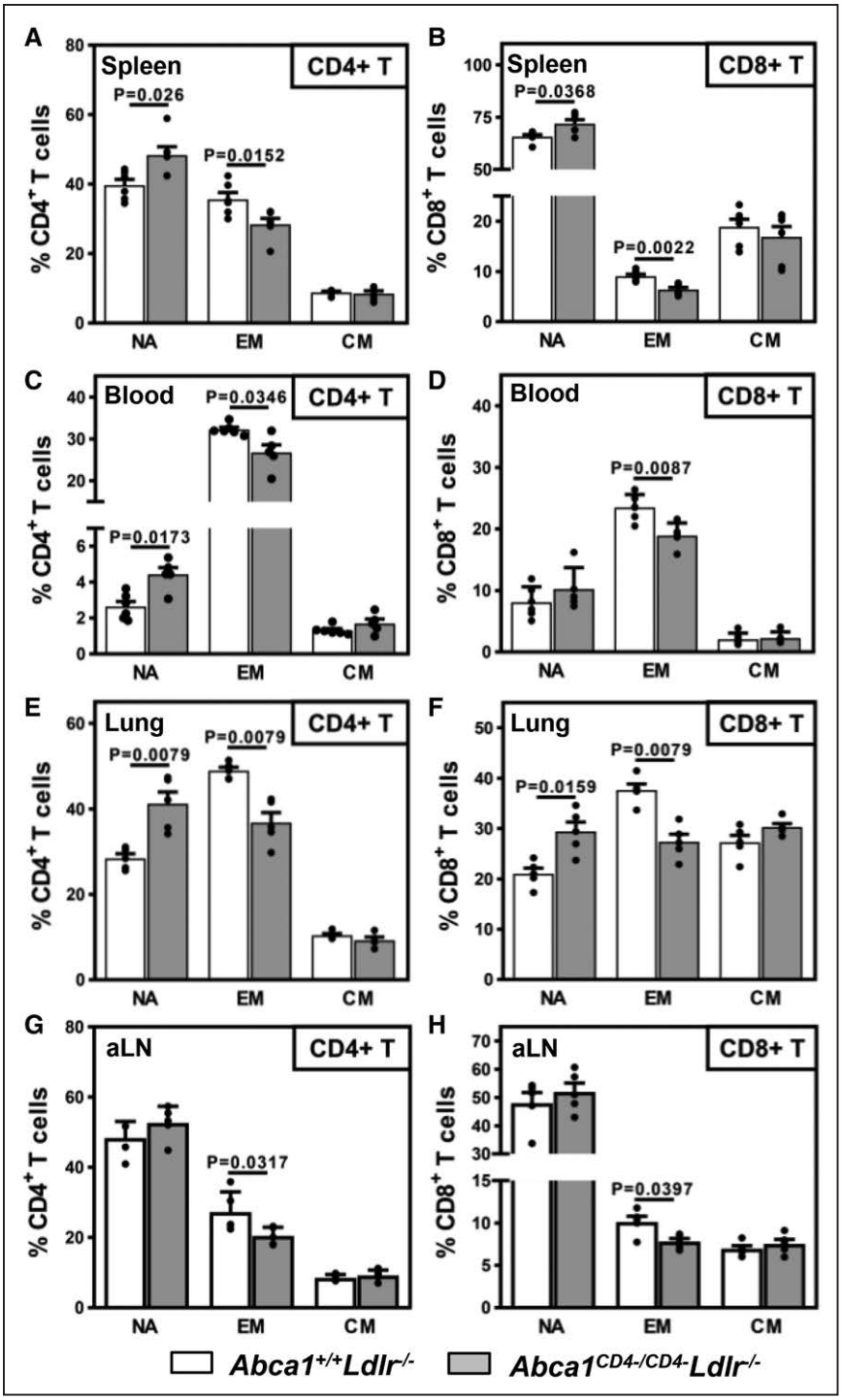

Figure 5. T-cell–specific deletion of ABCA1 (ATP-binding cassette transporter A1) specifically decreases the number of effector memory (EM) T cells in Ldlr$^{-/-}$mice on Western-type diet (WTD).
After feeding with WTD for 9 weeks, percentages of CD62L^{+}CD44^{-} naive (NA), CD62L^{-}CD44^{+} EM, and CD62L^{+}CD44^{+} CM T cells within gated CD4^{+} (**A**, **C**, **E**, and **G**) or CD8^{+} (**B**, **D**, **F**, and **H**) T cell compartment in indicated tissues of female *Abca1*$^{CD4-/CD4-}$*Ldlr*$^{-/-}$ (gray bar) and *Abca1*$^{+/+}$*Ldlr*$^{-/-}$ (open bar) mice were analyzed by fluorescence-activated cell sorting (FACS). The absolute numbers of total leukocytes did not differ significantly in corresponding tissues of the 2 groups (Figure S4C through S4F). Data are expressed as mean±SEM (n=5–6/group). Results were compared with unpaired Mann-Whitney *U* test. aLN indicates aortic lymph nodes.

DISCUSSION

ABCA1 plays a critical role in reverse cholesterol transport by facilitating HDL biogenesis and stimulating cellular cholesterol efflux. Although macrophage reverse cholesterol transport greatly affects the formation of foam cells in atherosclerotic lesions, specific deletion of ABCA1 in mature macrophages/neutrophils has little impact on the development of atherosclerotic lesions.[11] Nevertheless, the atheroprotective effects of hematopoietic ABCA1 were consistently observed in bone marrow transplantation studies,[7–9] regardless of the expression of LDLr (low-density lipoprotein receptor) on hematopoietic cells.[24] Therefore, the type of cells responsible for bone marrow ABCA1-mediated atheroprotection remains elusive so far. In the current study, we, for the first time to our knowledge, investigated the roles of T-cell ABCA1 on atherosclerosis. To our surprise, specific deletion of ABCA1 in T cells alleviates atherosclerosis in both male and female mice. Mechanistically, ablation of ABCA1

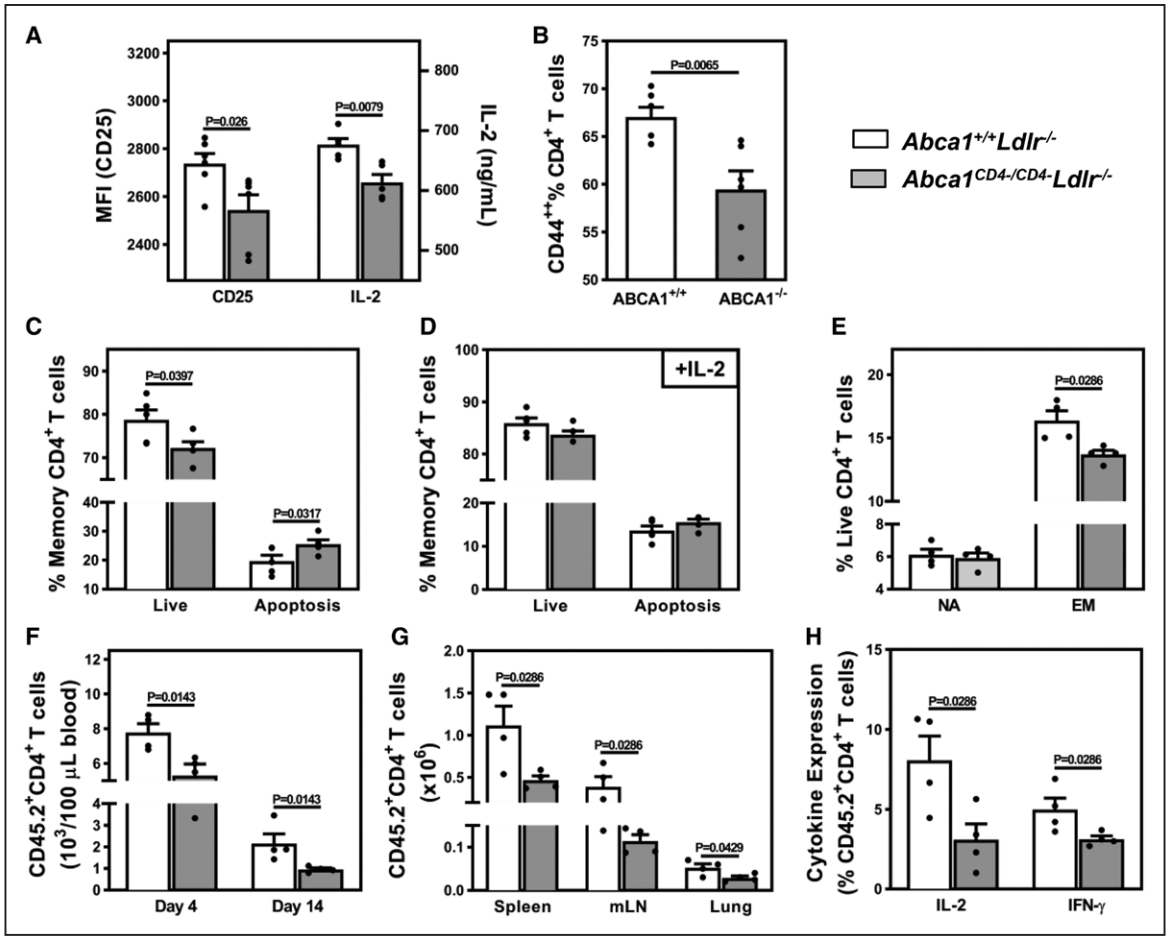

Figure 6. ABCA1 (ATP-binding cassette transporter A1) deficiency reduces the generation and survival of CD4⁺ memory T cells both in vitro and in vivo.

Naive CD62L⁺CD44⁻CD4⁺ T cells were purified from spleens of female *Abca1*$^{CD4-/CD4-}$*Ldlr*$^{-/-}$ (gray bar) and *Abca1*$^{+/+}$*Ldlr*$^{-/-}$ (open bar) mice on normal laboratory diet (NLD; n=5–6 mice/group), and were subsequently stimulated with 1 µg/mL plate-bound α-CD3 and soluble α-CD28 antibodies in vitro. **A**, Levels of CD25 on cell surface or IL (interleukin)-2 in supernatants after 24 hours' stimulation. **B**, Percents of CD44⁺⁺CD4⁺ T cells after 72 hours' stimulation. **C** and **D**, Percentages of live (Annexin V⁻7-AAD⁻) or apoptotic (Annexin V⁺) cells after a further 3-day culture of fluorescence-activated cell sorting (FACS)-sorted CD4⁺CD44⁺⁺ memory T cells (72 hours post the primary stimulation) in the absence (**C**) or presence (**D**) of 10 ng/mL of exogenous IL-2. **E**, Percents of live cells after a 3-day culture of FACS-purified naive (NA) or effector memory (EM) CD4⁺T cells from spleens of female *Abca1*$^{CD4-/CD4-}$*Ldlr*$^{-/-}$ or *Abca1*$^{+/+}$*Ldlr*$^{-/-}$ mice on NLD (n=4 mice/group). **F** and **G**, Numbers of donor-derived CD45.2⁺CD4⁺OT-II T cells in the blood (**F**) or indicated tissues (**G**) of CD45.1⁺ recipients. **H**, Percentages of IL-2⁺ or IFN (interferon)-γ⁺ cells within gated CD4⁺CD45.2⁺ memory T cells after restimulation with the $OVA_{323-339}$ peptide on day 14 post immunization. Naive CD4⁺CD62L⁺CD44⁻ T cells, purified from spleens of male *Abca1*$^{CD4-/CD4-}$OT-II (gray bar) or *Abca1*$^{+/+}$OT-II (open bar) mice (CD45.2⁺) on NLD, were injected into CD45.1⁺ congenic female recipient mice (n=4 mice/group), which were immunized with OVA plus lipopolysaccharide 24 hours later (**F**–**H**). Data are expressed as mean±SEM. All results were compared with unpaired Mann-Whitney *U* test. *P* values in **F**–**H** were calculated by 1-tailed test. MFI indicates mean fluorescence intensity; and mLN, mesenteric lymph nodes.

attenuates TCR signaling, suppresses the formation and function of EM T cells, and significantly reduces arterial T cell accumulations in response to hypercholesterolemia, thereby ameliorating the development of atherosclerosis in *Ldlr*$^{-/-}$ mice.

Cholesterol is a key component of cell membranes and is especially enriched in lipid rafts. Membrane cholesterol depletion using methyl-β-cyclodextrin results in a disruption of lipid rafts in T cells.[25] We show here that ABCA1 plays a critical role in cholesterol homeostasis of T cells as its deficiency not only remarkably inhibits apo AI–mediated cholesterol efflux, but also slightly reduces cholesterol outflow to HDL. Strikingly, contrary to the increased content of lipid rafts in ABCA1-deficient macrophages,[26] ABCA1-deficient T cells exhibit a slight but consistent decrease in membrane lipid rafts, implying substantially different contributions of ABCA1-mediated cholesterol efflux in the formation of membrane lipid rafts between these two cell types. Indeed, unlike macrophages with high levels of ABCA1,[8] T cells express 5 times less ABCA1 than ABCG1, and the latter is further upregulated upon ABCA1 deletion. ABCG1, a direct target of LXR β induced by intracellular cholesterol derivates,[15] is preferentially localized in Triton X-100 resistant raft domains and mediates the efflux of both cholesterol and cholesterol-associated sphingomyelin.[27,28] Given the

significantly higher expression of ABCG1 in T cells, and the elevated levels of cellular cholesterol and membrane lipid rafts in ABCG1-deficient CD4+ T cells,[17] it seems that T cells rely more on ABCG1, rather than ABCA1, to maintain the homeostasis of cellular cholesterol and membrane lipid rafts. In this scenario, the slightly decreased membrane lipid rafts in ABCA1-deficient T cells are likely attributable to the increased ABCG1, which promotes the efflux of cholesterol and sphingomyelin and eventually reduces the contents of lipid rafts in T-cell membranes. Importantly, increased lipid rafts in ABCG1-deficient T cells enhance TCR signaling,[17] while downregulation of lipid rafts by depletion of cholesterol or sphingomyelin inhibits the multimerization of TCR and thereby sequestrates its signaling.[25,29,30] It is thus conceivable that the impaired TCR signaling in ABCA1-deficient T cells, manifested by decreased phosphorylation of ZAP70 and ERK upon activation in vitro, is partially due to ABCG1 upregulation and the subsequent reduction of membrane raft domains.

Despite little impact on thymic T-cell development and the number/phenotype of mature T cells in the periphery under homeostatic conditions on NLD, deletion of ABCA1 profoundly hampers the survival, proliferation, and function of conventional T cells both in vitro and in vivo, likely owing to the impaired TCR signaling.[31] Upon TCR triggering, ABCA1-deficient CD4+ T cells produce less IL-2 and express reduced levels of its receptor α chain CD25 on the cell surface. Given the essential role of IL-2 in the survival, long-term proliferation, and differentiation of activated T cells,[32,33] the impaired IL-2/CD25 pathway in ABCA1-deficient T cells may further amplify their TCR signaling defects, resulting in increased apoptosis, reduced proliferation, and differentiation towards memory T cells as well as impaired functionality. Apart from conventional T cells, cholesterol metabolism regulates Treg cell homeostasis as well.[34] Hypercholesterolemia increases the Treg population,[35,36] while oxidized LDL dampens the number and suppressive ability of Treg cells.[37] As ABCA1 is expressed in Treg cells and apo AI restores the in vitro Treg differentiation repressed by oxLDL,[38,39] an important role of ABCA1 in Treg cell biology has been postulated. However, our data here demonstrated that specific deletion of ABCA1 in T cells has little impact on the number and suppressive function of peripheral Treg cells, even under hypercholesterolemia. The negative effect of ABCA1-deficiency on Treg cells might be (partially) compensated by the activation of LXRβ, illustrated by upregulated downstream molecule ABCG1, because decreased/increased LXRβ activity disrupts/promotes the differentiation, fitness, and function of Treg cells, respectively, in a cell-autonomous fashion.[40,41] Likewise, the aberrantly augmented LXRβ and ABCG1 may also contribute to the impaired proliferation, differentiation, and effector function of conventional T cells lacking ABCA1.[15,17,41] Indeed, the activation and proliferation defects of ABCA1-knockout T cells were completely reversed by compound deletions of both ABCA1 and ABCG1 (unpublished data).

During atherogenesis, antigens, generated as a consequence of hypercholesterolemia, trigger the activations of naive T cells, some of which will differentiate into either central memory or EM T cells. Central memory T cells are preferentially home to lymphoid organs, while EM T cells express tissue-homing receptors associated with inflammation, such as CCR5 and CXCR3, and exert effector functions more readily. Of note, memory, especially EM, T cells are shown to be associated with atherosclerosis or coronary artery disease in humans and animal models.[42,43] CD4+ and CD8+ T cells aggravate atherosclerosis development mainly via IFN-γ[44-46]. Moreover, CD8+ T cells may also promote lesion progression by inducing the apoptosis of macrophages in plaques which subsequently attracts more proinflammatory macrophages.[47] In line with these findings, mice with T-cell–specific ABCA1-deficiency on an *Ldlr*$^{-/-}$background, after 9-week feeding of WTD, showed significantly less accumulations of T cells in plaques and surrounding adventitias, and more importantly, ameliorated atherosclerotic lesions than the *Abca1*$^{+/+}$ littermates. The vascular accumulations of T cells mainly result from the infiltration of T cells as well as their subsequent expansion in situ. It has been reported that antagonizing the function of CCR5 and CXCR3 by small molecules almost completely blocks the influx of T cells into atherosclerotic plaques (≈ 95%) and thereby greatly attenuates atherogenesis in *Ldlr*$^{-/-}$ mice.[48] Hence, the significantly reduced levels of CXCR3 and CCR5 on ABCA1$^{-/-}$ T cells, both in vitro upon activation and in vivo after WTD feeding, indicate that the hampered infiltration of T cells contributes significantly to their decreased numbers in lesions in *Abca1*$^{CD4-/CD4-}$*Ldlr*$^{-/-}$mice. Given that IFN-γ promotes the expression of CXCR3 and CCR5 on T cells,[49,50] it is conceivable that the following cause-effect relationship exists: depletion of ABCA1 inhibits IFN-γ production via impairing TCR signaling, thereby repressing CXCR3 and CCR5 expression on T cells and their subsequent migration toward inflammatory lesions/vessels, eventually leading to mitigated atherosclerotic plaque formations. In addition, the reduced survival, expansion, and IFN-γ–producing ability of infiltrated ABCA1-deficient T cells in adventitias and plaques contribute to the diminished atherogenesis as well.

Although CD8+ T-cell immunity may depend on CD4+ T-cell help in some pathological conditions,[51] deletion of ABCA1 exerts a similar impact on the number, phenotype, and function of CD4+ or CD8+ T cells in vitro and in vivo. It is thus difficult to ascertain the relative contribution of CD4+ versus CD8+ T cells to T-cell–specific ABCA1-mediated atherogenesis in the current study, which might be achieved, for instance, by adoptive transfer of mature

control CD4+ plus ABCA1-deficient CD8+ T cells (or *vice versa*) into nude mice on an *Ldlr*$^{-/-}$ background.

Recently, Cheng et al[18] revealed that specific deletion of ABCG1 in T cells increases the intracellular cholesterol content, enhances the differentiation of naive CD4+ T cells into Foxp3+ Treg cells, and thereby protects *Ldlr*$^{-/-}$ mice against atherosclerosis. Interestingly, augmented cholesterol efflux to apo AI via ABCA1 reduces cellular cholesterol levels in Treg cells and inhibits their conversion into T follicular helper cells during atherogenesis.[39] Thus, it appears that cholesterol levels play distinct roles in the differentiation versus stability of Treg cells. Here we found that deletion of ABCA1 in T cells did not significantly affect the number and function of Treg cells, which may relate to the fact that on one hand, T cells, as discussed above, depend more on ABCG1 for cholesterol homeostasis; and on the other hand, the upregulated ABCG1 compensates for the loss of ABCA1 in maintaining intracellular cholesterol levels. Nevertheless, although modulation of T cell cholesterol homeostasis by deletion of either ABCA1 or ABCG1 is atheroprotective, the underlying mechanisms differ substantially as ABCA1 functions through conventional T cells while the latter acts mainly via Treg cells.

Notably, the cell-intrinsic effects of ABCA1 on T-cell biology and atherosclerosis development seem to be gender-independent. T-cell–specific depletions of ABCA1 similarly impact the phenotype and function of T cells in male or female mice, and thereby significantly mitigate the development of atherosclerotic lesions in both genders. Although most of our in vitro experiments were performed on cells isolated from female mice, ABCA1-deficient OT-II CD4+ T cells isolated from male mice exhibit not only an attenuated TCR signaling upon activation in vitro, but also an impaired generation/survival of memory T cells as well as a reduced functionality upon transfer in vivo.

In summary, our results show that specific deletion of ABCA1 in T cells impairs TCR signaling, inhibits the activation, survival, proliferation of T cells and the formation of EM T cells, leading to significantly reduced accumulation of T cells in lesions and attenuated atherogenesis. To our knowledge, this is the first direct evidence showing cell-intrinsic roles of ABCA1 in T cell biology and atherosclerosis.

ARTICLE INFORMATION

Received October 8, 2020; accepted September 27, 2022.

Affiliations

Department of Pathophysiology (Y.Z., L.Z., L.L., F.D., Y.Y., S.D.), Department of Immunology (X.Z.), School of Biology & Basic Medical Sciences, and Institutes of Biology & Medical Sciences (H.W., J.W.), Soochow Medical College of Soochow University, Suzhou, China. Division of BioTherapeutics (M.V.E.) and Division of Systems Pharmacology and Pharmacy (M.V.E.), Leiden Academic Centre for Drug Research, Leiden University, the Netherlands. Pharmacy Leiden, the Netherlands (M.V.E.).

Sources of Funding

This study was financially supported by National Natural Science Foundation of China (81470564/81970371 [Y. Zhao] and 32170914/31670888 [J. Wang]); Priority Academic Program Development of Jiangsu Higher Education Institutions (J. Wang and Y. Zhao). M. Van Eck is supported by a VICI grant (91813603) from the Netherlands Organization for Scientific Research and is an Established Investigator of the Dutch Heart Foundation (2007T056). The funders had no roles in the study design, data collection and analysis, decision to publish, or preparation of the article.

Disclosures

None.

Supplemental Material

Table S1
Figures S1–S6
Major Resources Table

REFERENCES

1. Zhao Y, Van Berkel TJ, Van Eck M. Relative roles of various efflux pathways in net cholesterol efflux from macrophage foam cells in atherosclerotic lesions. *Curr Opin Lipidol.* 2010;21:441–453. doi: 10.1097/MOL.0b013e32833dedaa
2. Oram JF, Vaughan AM. ABCA1-mediated transport of cellular cholesterol and phospholipids to HDL apolipoproteins. *Curr Opin Lipidol.* 2000;11:253–260. doi: 10.1097/00041433-200006000-00005
3. Aiello RJ, Brees D, Bourassa PA, Royer L, Lindsey S, Coskran T, Haghpassand M, Francone OL. Increased atherosclerosis in hyperlipidemic mice with inactivation of ABCA1 in macrophages. *Arterioscler Thromb Vasc Biol.* 2002;22:630–637. doi: 10.1161/01.atv.0000014804.35824.da
4. Singaraja RR, Van Eck M, Bissada N, Zimetti F, Collins HL, Hildebrand RB, Hayden A, Brunham LR, Kang MH, Fruchart J, et al. Both hepatic and extrahepatic ABCA1 have discrete and essential functions in the maintenance of plasma high-density lipoprotein cholesterol levels in vivo. *Circulation.* 2006;114:1301–1309. doi: 10.1161/CIRCULATIONAHA.106.621433
5. Brunham LR, Kruit JK, Iqbal J, Fievet C, Timmins JM, Pape TD, Coburn BA, Bissada N, Staels B, Groen AK, et al. Intestinal ABCA1 directly contributes to HDL biogenesis in vivo. *J Clin Invest.* 2006;116:1052–1062. doi: 10.1172/JCI27352
6. Chung S, Sawyer JK, Gebre AK, Maeda N, Parks JS. Adipose tissue ATP binding cassette transporter A1 contributes to high-density lipoprotein biogenesis in vivo. *Circulation.* 2011;124:1663–1672. doi: 10.1161/CIRCULATIONAHA.111.025445
7. van Eck M, Bos IS, Kaminski WE, Orsó E, Rothe G, Twisk J, Böttcher A, Van Amersfoort ES, Christiansen-Weber TA, Fung-Leung WP, et al. Leukocyte ABCA1 controls susceptibility to atherosclerosis and macrophage recruitment into tissues. *Proc Natl Acad Sci USA.* 2002;99:6298–6303. doi: 10.1073/pnas.092327399
8. Zhao Y, Pennings M, Hildebrand RB, Ye D, Calpe-Berdiel L, Out R, Kjerrulf M, Hurt-Camejo E, Groen AK, Hoekstra M, et al. Enhanced foam cell formation, atherosclerotic lesion development, and inflammation by combined deletion of ABCA1 and SR-BI in Bone marrow-derived cells in LDL receptor knockout mice on western-type diet. *Circ Res.* 2010;107:e20–e31. doi: 10.1161/CIRCRESAHA.110.226282
9. Van Eck M, Singaraja RR, Ye D, Hildebrand RB, James ER, Hayden MR, Van Berkel TJ Macrophage ATP-binding cassette transporter A1 overexpression inhibits atherosclerotic lesion progression in low-density lipoprotein receptor knockout mice. *Arterioscler Thromb Vasc Biol.* 2006;26(4):929–934. doi: 10.1161/01.ATV.0000208364.22732.16
10. Brunham LR, Singaraja RR, Duong M, Timmins JM, Fievet C, Bissada N, Kang MH, Samra A, Fruchart JC, McManus B, et al. Tissue-specific roles of ABCA1 influence susceptibility to atherosclerosis. *Arterioscler Thromb Vasc Biol.* 2009;29:548–554. doi: 10.1161/ATVBAHA.108.182303
11. Bi X, Zhu X, Gao C, Shewale S, Cao Q, Liu M, Boudyguina E, Gebre AK, Wilson MD, Brown AL, et al. Myeloid cell-specific ATP-binding cassette transporter A1 deletion has minimal impact on atherogenesis in atherogenic diet-fed low-density lipoprotein receptor knockout mice. *Arterioscler Thromb Vasc Biol.* 2014;34:1888–1899. doi: 10.1161/ATVBAHA.114.303791
12. Libby P, Lichtman AH, Hansson GK. Immune effector mechanisms implicated in atherosclerosis: from mice to humans. *Immunity.* 2013;38:1092–1104. doi: 10.1016/j.immuni.2013.06.009

13. Pizzo P, Viola A. Lymphocyte lipid rafts: structure and function. *Curr Opin Immunol*. 2003;15:255–260. doi: 10.1016/s0952-7915(03)00038-4
14. Kidani Y, Bensinger SJ. Modulating cholesterol homeostasis to build a better t cell. *Cell Metab*. 2016;23:963–964. doi: 10.1016/j.cmet.2016.05.015
15. Bensinger SJ, Bradley MN, Joseph SB, Zelcer N, Janssen EM, Hausner MA, Shih R, Parks JS, Edwards PA, Jamieson BD, et al. LXR signaling couples sterol metabolism to proliferation in the acquired immune response. *Cell*. 2008;134:97–111. doi: 10.1016/j.cell.2008.04.052
16. Kidani Y, Elsaesser H, Hock MB, Vergnes L, Williams KJ, Argus JP, Marbois BN, Komisopoulou E, Wilson EB, Osborne TF, et al. Sterol regulatory element-binding proteins are essential for the metabolic programming of effector T cells and adaptive immunity. *Nat Immunol*. 2013;14:489–499. doi: 10.1038/ni.2570
17. Armstrong AJ, Gebre AK, Parks JS, Hedrick CC. ATP-binding cassette transporter G1 negatively regulates thymocyte and peripheral lymphocyte proliferation. *J Immunol*. 2010;184:173–183. doi: 10.4049/jimmunol.0902372
18. Cheng HY, Gaddis DE, Wu R, McSkimming C, Haynes LD, Taylor AM, McNamara CA, Sorci-Thomas M, Hedrick CC. Loss of ABCG1 influences regulatory T cell differentiation and atherosclerosis. *J Clin Invest*. 2016;126:3236–3246. doi: 10.1172/JCI83136
19. Sankaranarayanan S, Kellner-Weibel G, de la Llera-Moya M, Phillips MC, Asztalos BF, Bittman R, Rothblat GH. A sensitive assay for ABCA1-mediated cholesterol efflux using BODIPY-cholesterol. *J Lipid Res*. 2011;52:2332–2340. doi: 10.1194/jlr.D018051
20. Du XM, Kim MJ, Hou L, Le Goff W, Chapman MJ, Van Eck M, Curtiss LK, Burnett JR, Cartland SP, Quinn CM, et al. HDL particle size is a critical determinant of ABCA1-mediated macrophage cellular cholesterol export. *Circ Res*. 2015;116:1133–1142. doi: 10.1161/CIRCRESAHA.116.305485
21. Soroosh P, Ine S, Sugamura K, Ishii N. Differential requirements for OX40 signals on generation of effector and central memory CD4+ T cells. *J Immunol*. 2007;179:5014–5023. doi: 10.4049/jimmunol.179.8.5014
22. Damoiseaux J. The IL-2 - IL-2 receptor pathway in health and disease: The role of the soluble IL-2 receptor. *Clin Immunol*. 2020;218:108515. doi: 10.1016/j.clim.2020.108515
23. Cheng ZY, He TT, Gao XM, Zhao Y, Wang J. ZBTB transcription factors: key regulators of the development, differentiation and effector function of T cells. *Front Immunol*. 2021;12:713294. doi: 10.3389/fimmu.2021.713294
24. Ouweneel AB, Zhao Y, Calpe-Berdiel L, Lammers B, Hoekstra M, Van Berkel TJC, Van Eck M. Impact of bone marrow ATP-binding cassette transporter A1 deficiency on atherogenesis is independent of the presence of the low-density lipoprotein receptor. *Atherosclerosis*. 2021;319:79–85. doi: 10.1016/j.atherosclerosis.2021.01.001
25. Kabouridis PS, Janzen J, Magee AL, Ley SC. Cholesterol depletion disrupts lipid rafts and modulates the activity of multiple signaling pathways in T lymphocytes. *Eur J Immunol*. 2000;30:954–963. doi: 10.1002/1521-4141(200003)30:3<954::AID-IMMU954>3.0.CO;2-Y
26. Zhu X, Lee JY, Timmins JM, Brown JM, Boudyguina E, Mulya A, Gebre AK, Willingham MC, Hiltbold EM, Mishra N, et al. Increased cellular free cholesterol in macrophage-specific Abca1 knock-out mice enhances pro-inflammatory response of macrophages. *J Biol Chem*. 2008;283:22930–22941. doi: 10.1074/jbc.M801408200
27. Sano O, Kobayashi A, Nagao K, Kumagai K, Kioka N, Hanada K, Ueda K, Matsuo M. Sphingomyelin-dependence of cholesterol efflux mediated by ABCG1. *J Lipid Res*. 2007;48:2377–2384. doi: 10.1194/jlr.M700139-JLR200
28. Sano O, Ito S, Kato R, Shimizu Y, Kobayashi A, Kimura Y, Kioka N, Hanada K, Ueda K, Matsuo M. ABCA1, ABCG1, and ABCG4 are distributed to distinct membrane meso-domains and disturb detergent-resistant domains on the plasma membrane. *PLoS One*. 2014;9:e109886. doi: 10.1371/journal.pone.0109886
29. Molnár E, Swamy M, Holzer M, Beck-García K, Worch R, Thiele C, Guigas G, Boye K, Luescher IF, Schwille P, et al. Cholesterol and sphingomyelin drive ligand-independent T-cell antigen receptor nanoclustering. *J Biol Chem*. 2012;287:42664–42674. doi: 10.1074/jbc.M112.386045
30. Jin ZX, Huang CR, Dong L, Goda S, Kawanami T, Sawaki T, Sakai T, Tong XP, Masaki Y, Fukushima T, et al. Impaired TCR signaling through dysfunction of lipid rafts in sphingomyelin synthase 1 (SMS1)-knockdown T cells. *Int Immunol*. 2008;20:1427–1437. doi: 10.1093/intimm/dxn100
31. Bhattacharyya ND, Feng CG. Regulation of T Helper Cell Fate by TCR Signal Strength. *Front Immunol*. 2020;11:624. doi: 10.3389/fimmu.2020.00624
32. Deenick EK, Gett AV, Hodgkin PD. Stochastic model of T cell proliferation: a calculus revealing IL-2 regulation of precursor frequencies, cell cycle time, and survival. *J Immunol*. 2003;170:4963–4972. doi: 10.4049/jimmunol.170.10.4963
33. Hedfors IA, Brinchmann JE. Long-term proliferation and survival of in vitro-activated T cells is dependent on Interleukin-2 receptor signaling but not on the high-affinity IL-2R. *Scand J Immunol*. 2003;58:522–532. doi: 10.1046/j.1365-3083.2003.01338.x
34. Pinzon Grimaldos A, Bini S, Pacella I, Rossi A, Di Costanzo A, Minicocci I, D'Erasmo L, Arca M, Piconese S. The role of lipid metabolism in shaping the expansion and the function of regulatory T cells. *Clin Exp Immunol*. 2022;208:181–192. doi: 10.1093/cei/uxab033
35. Maganto-García E, Tarrio ML, Grabie N, Bu DX, Lichtman AH. Dynamic changes in regulatory T cells are linked to levels of diet-induced hypercholesterolemia. *Circulation*. 2011;124:185–195. doi: 10.1161/CIRCULATIONAHA.110.006411
36. Mailer RKW, Gisterå A, Polyzos KA, Ketelhuth DFJ, Hansson GK. Hypercholesterolemia enhances t cell receptor signaling and increases the regulatory t cell population. *Sci Rep*. 2017;7:15655. doi: 10.1038/s41598-017-15546-8
37. Mor A, Luboshits G, Planer D, Keren G, George J. Altered status of $CD4^+CD25^+$ regulatory T cells in patients with acute coronary syndromes. *Eur Heart J*. 2006;27:2530–2537. doi: 10.1093/eurheartj/ehl222
38. Wilhelm AJ, Zabalawi M, Owen JS, Shah D, Grayson JM, Major AS, Bhat S, GibbsThomas DPMJ, Sorci-Thomas MG. Apolipoprotein A-I modulates regulatory T cells in autoimmune $LDLr^{-/-}$, $ApoA\text{-}I^{-/-}$ mice. *J Biol Chem*. 2010;285:36158–36169. doi: 10.1074/jbc.M110.134130.
39. Gaddis DE, Padgett LE, Wu R, McSkimming C, Romines V, Taylor AM, McNamara CA, Kronenberg M, Crotty S, Thomas MJ, et al. Apolipoprotein AI prevents regulatory to follicular helper T cell switching during atherosclerosis. *Nat Commun*. 2018;9:1095. doi: 10.1038/s41467-018-03493-5
40. Herold M, Breuer J, Hucke S, Knolle P, Schwab N, Wiendl H, Klotz L. Liver X receptor activation promotes differentiation of regulatory T cells. *PLoS One*. 2017;12:e0184985. doi: 10.1371/journal.pone.0184985
41. Michaels AJ, Campbell C, Bou-Puerto R, Rudensky AY. Nuclear receptor LXRβ controls fitness and functionality of activated T cells. *J Exp Med*. 2021;218:e20201311. doi: 10.1084/jem.20201311
42. Ammirati E, Cianflone D, Vecchio V, Banfi M, Vermi AC, De Metrio M, Grigore L, Pellegatta F, Pirillo A, Garlaschelli K, et al. Effector memory t cells are associated with atherosclerosis in humans and animal models. *J Am Heart Assoc*. 2012;1:27–41. doi: 10.1161/JAHA.111.000125
43. Olson NC, Doyle MF, Jenny NS, Huber SA, Psaty BM, Kronmal RA, Tracy RP. Decreased naive and increased memory CD4(+) T cells are associated with subclinical atherosclerosis: the multi-ethnic study of atherosclerosis. *PLoS One*. 2013;8:e71498. doi: 10.1371/journal.pone.0071498
44. Ketelhuth DF, Hansson GK. Adaptive response of t and b cells in atherosclerosis. *Circ Res*. 2016;118:668–678. doi: 10.1161/CIRCRESAHA.115.306427
45. Gupta S, Pablo AM, Jiang XC, Wang N, Tall AR, Schindler C. IFN-gamma potentiates atherosclerosis in ApoE knock-out mice. *J Clin Invest*. 1997;99:2752–2761. doi: 10.1172/JCI119465
46. van Duijn J, Kuiper J, Slütter B. The many faces of CD8+ T cells in atherosclerosis. *Curr Opin Lipidol*. 2018;29:411–416. doi: 10.1097/MOL.0000000000000541
47. Seijkens TTP, Poels K, Meiler S, van Tiel CM, Kusters PJH, Reiche M, Atzler D, Winkels H, Tjwa M, Poelman H, et al. Deficiency of the T cell regulator Casitas B-cell lymphoma-B aggravates atherosclerosis by inducing CD8+ T cell–mediated macrophage death. *Eur Heart J*. 2019;40:372–382. doi: 10.1093/eurheartj/ehy714
48. van Wanrooij EJ, Happé H, Hauer AD, de Vos P, Imanishi T, Fujiwara H, van Berkel TJ, Kuiper J. HIV entry inhibitor TAK-779 attenuates atherogenesis in low-density lipoprotein receptor-deficient mice. *Arterioscler Thromb Vasc Biol*. 2005;25:2642–2647. doi: 10.1161/01.ATV.0000192018.90021.c0
49. Nakajima C, Mukai T, Yamaguchi N, Morimoto Y, Park WR, Iwasaki M, Gao P, Ono S, Fujiwara H, Hamaoka T. Induction of the chemokine receptor CXCR3 on TCR-stimulated T cells: dependence on the release from persistent TCR-triggering and requirement for IFN-gamma stimulation. *Eur J Immunol*. 2002;32:1792–1801. doi: 10.1002/1521-4141(200206)32:6<1792::AID-IMMU1792>3.0.CO;2-0
50. Iwasaki M, Mukai T, Nakajima C, Yang YF, Gao P, Yamaguchi N, Tomura M, Fujiwara H, Hamaoka T. A mandatory role for STAT4 in IL-12 induction of mouse T cell CCR5. *J Immunol*. 2001;167:6877–6883. doi: 10.4049/jimmunol.167.12.6877
51. Bedoui S, Heath WR, Mueller SN. CD4(+) T-cell help amplifies innate signals for primary CD8(+) T-cell immunity. *Immunol Rev*. 2016;272:52–64. doi: 10.1111/imr.12426